MANUFACTURING OF FIRE RESISTANT POROUS Ca-SILICATE CERAMICS

A Thesis Submitted to
the Graduate School of Engineering and Sciences of
İzmir Institute of Technology
in Partial Fulfillment of the Requirements for the Degree of
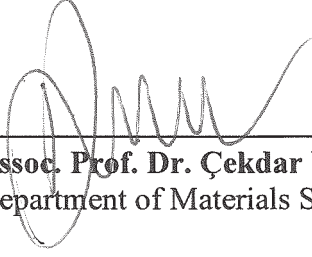
MASTER OF SCIENCE

in Materials Science and Engineering

by
Ezgi OĞUR

December 2019
İZMİR
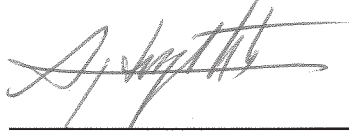
We approve the thesis of **Ezgi OĞUR**

Examining Committee Members:

_____
Assoc. Prof. Dr. Çekdar Vakıf AHMETOĞLU
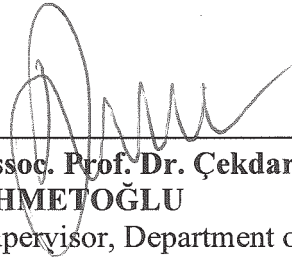Department of Materials Science and Engineering, İzmir Institute of Technology

_____
Assoc. Prof. Dr. Yaşar AKDOĞAN
Department of Materials Science and Engineering, İzmir Institute of Technology

_____
Prof. Dr. Ali Aydın GÖKTAŞ
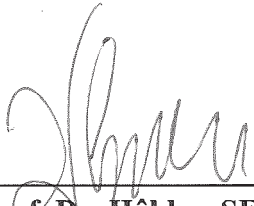Department of Metallurgy and Materials Engineering, Dokuz Eylül University

19 December 2019

_____
Assoc. Prof. Dr. Çekdar Vakıf AHMETOĞLU
Supervisor, Department of Materials
Science and Engineering,
İzmir Institute of Technology

_____
Asst. Prof. Dr. Umut ADEM
Co-Supervisor, Department of
Materials Science and Engineering,
İzmir Institute of Technology

_____
Prof. Dr. Hâldun SEVİNÇLİ
Head of the Department of Materials
Science and Engineering
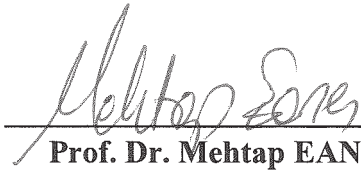
_____
Prof. Dr. Mehtap EANES
Dean of the Graduate School of
Engineering and Science

ACKNOWLEDGMENTS

ABSTRACT

MANUFACTURING OF FIRE RESISTANT POROUS Ca-SILICATE CERAMICS

Calcium silicate hydrates are a group of materials belonging to the calcium silicate family. Calcium silicate hydrates are crucial materials in the building industry, especially for thermal insulation and fire-resistant applications. Tobermorite and xonotlite, calcium silicate hydrates, are the most popular materials in the literature due to their structural properties. These material are synthesized by hydrothermal processes. In some publications, several pre-treatments are applied to the starting materials before hydrothermal synthesis. In this thesis, the effects of these processes on different starting materials and how does changing the parameters affect the process are examined. Besides, the main objective of the thesis is to produce the xonotlite phase using recycling materials as economically as possible. Calcium silicate hydrates powders containing approximately 61 wt. % xonotlite was produced with using lime and recycled glass by hydrothermal synthesis method. The obtained product has a mainly fibrous morphology due to the main phase is xonotlite. According to phase analysis, tobermorite, scawtite, and the trace of calcite phases are also present in the general structure. The thermogravimetric analysis demonstrated that approximately 20% loss is observed up to 800°C (at about that temperature transformation of the xonotlite to the wollastonite phase is occur.). The mass change remained constant between 800°C and 1200°C. Calcium silicate powder (obtained by thermal treatments from CSH) was also thermally analyzed and consequently remained stable up to 1200°C, (the loss was approximately <1%).

ÖZET

YANMAYA DAYANIKLI GÖZENEKLİ Ca-SİLİKAT SERAMİKLERİNİN GELİŞTİRİLMESİ

Kalsiyum silikat hidratlar kalsiyum silikat ailesine dahil bir malzeme grubudur. Kalsiyum silikat hidratlar yapı endüstrisinde özellikle ısı yalıtımı ve ateşe dayanıklı uygulamalar için çok önemli malzemelerdir. Kalsiyum silikat hidratlardan olan tobermorite ve xonotlite, yapısal özelliklerinden ötürü literatürde en çok ilgi gören malzemelerdir. Bu malzemeler hidrotermal süreçler ile sentezlenmektedir. Bazı yayınlarda hidrotermal sentezden önce, başlangıç malzemelerine birkaç ön-işlem uygulanmaktadır. Bu tezde de bu süreçler, farklı başlangıç malzemeleri ve süreci etkileyen parametrelerin değiştirilmesinin son ürüne etkisi incelenmiştir. Bunun dışında, tezin asıl amacı, xonotlite fazının geri dönüşüm malzemeleri kullanılarak, olabildiğince ekonomik yollarla üretilmesidir. Ağırlıkça yaklaşık %61 xonotlite içeren kalsiyum silikat hidrat tozları, kireç ve geri dönüştürülmüş cam kullanılarak hidrotermal sentez yöntemi ile üretilmiştir. Elde edilen ürün, ana fazın xonotlite olması nedeniyle esasen lifli bir morfolojiye sahiptir. Faz analizine göre, genel yapıda tobermorite, scawtite ve kalsit fazlarının izi de mevcuttur. Termogravimetrik analiz, 800˚C 'ye kadar yaklaşık % 20 civarında bir kayıp gözlemlendiğini göstermiştir (yaklaşık olarak bu sıcaklıkta xonotlite fazının wollastonite fazına dönüşümü gerçekleşir). Ağırlık değişimi 800˚C ile 1200˚C arasında sabit kalmıştır. Kalsiyum silikat tozu (CSH'den termal işlemlerle elde edilen) de termal olarak analiz edildi ve sonuç olarak 1200 ˚C 'ye kadar stabil kaldı (kayıp yaklaşık < %1 idi).

TABLE OF CONTENTS

LIST OF FIGURES

LIST OF TABLES

CHAPTER 1

INTRODUCTION

1.1. Motivation

Silicon, calcium and oxygen are some of the most abundant elements on the surface of the earth and in the atmosphere (the amounts present in the earth crust - 25%, 3%, 50%, respectively).[1] Calcium silicates (CSs) contains these elements in their crystal structure and this makes them accessible as raw materials. In addition, due to the characteristic features such as the relatively ease of producibility and economically acceptable levels according to their refractory properties, in recent years the interest in these materials has increased. The phases of CSs be located in the fields of building materials industry (especially in cement production),[2, 3] bio-ceramic materials[4] and materials that provide resistance to high temperatures (refractory materials).[5] Therefore, the number of scientific studies in the field of CS has increased.

CS family varies according to the chemical component ranges. Also, calcium silicate hydrates (CSHs) belong to the calcium silicate family. The ratio of chemical component is generally based on the molar ratio of calcium to silicon in the structure. For CSs and CSHs, this ratio is generally between 0.5 and 3.0 .[6] On the periodic table instead of Ca metal, in the alkali metals and alkaline earth metals group elements such as Mg, Al and Na can be substituted in the structure[5, 7].

In the case of scientific publications, the production methods for CSs includes solid-state reactions, as well as ongoing heat treatment at various temperatures such as combustion, co-precipitation, sol-gel, etc.[8-11] For CSHs this method is generally hydrothermal synthesis. There are also studies about hydrothermal synthesis followed by mixing with ball-milling at room temperature called mechanochemical,[12, 13] or micro emulsion techniques.[14, 15] In the study, the afwillite [$Ca_3(SiO_3(OH))_2 \cdot 2H_2O$] phase from the CSHs was obtained by mechanochemical method and tobermorite was obtained by adding water to the system; however, it was observed that the tobermorite phase was

obtained with lower crystallinity compared to the tobermorite sample obtained by hydrothermal synthesis[16]. Another CSH production method with hydrothermal synthesis is used the supercritical behavior of water[17] on a certain temperature and pressure (T> 374˚C, P> 22 MPa-this behavior of water is intended to increase the reaction kinetics) using a continuous flow reactor[18, 19]. The hydrothermal synthesis method, which is the main CSH production method, will be discussed in detail later. However, this thesis is aimed to synthesize CS and CSHs in order to produce fire-resistant material which is a sub-branch of refractory materials.

1.2. Refractory Materials

Refractories are a group of materials that can withstand high loads under high temperatures. They are also resistant to mechanical loads and impacts, to abrasion and corrosion, and destructive factors such as thermal stress and thermal shock. Refractories must isolate the system during the process and protect the system from erosion/corrosion against process conditions. They are mainly made of non-metallic minerals/materials.

A very recent book by Ritwik Sarkar[20] provides comprehensive information on the refractory fundamentals and the applications, the interested reader is referred to this extensive work. Below only a brief overview will be mentioned for few compositions and their properties will be given in Table 1.1. Refractories can be classified into two sections; according to their chemical structures and their manufacturing methods. Also, there is a special case study; ceramic fibers will be discussed at the end of this section.[20]

1.2.1. Chemistry of the Refractories

Refractories can be classified as acidic, basic and neutral depending on their chemical structure. This classification is important as it is a gauge of how the refractory will behave in an environment.[20]

1.2.1.1. Acidic Refractories

Acidic refractories are resistant to acidic environments such as gas and slag at high temperatures. These refractories are only suitable for use in acidic environments (slag or

atmosphere). They are easily devastated by a reaction with any alkaline medium. Examples of these refractories are silica (SiO_2) and fireclay. In a basic environment, the refractory containing silica reacts with the basic medium and forms of silicates. Silicates also have a low melting point and react to more refractory material, resulting in material loss. Therefore, they are more suitable for use in acidic environments.[20]

1.2.1.2. Basic Refractories

Basic refractories are materials that are resistant to alkali environments at high temperatures. They are easy to be destroyed by acidic components and environments. Since basic refractories do not react with alkali slag, they are widely used in non-ferrous metallurgical processes and at cement production. Examples for these refractories are magnesia (MgO) and dolomi ($CaO.MgO$).[20]

1.2.1.3. Neutral Refractories

Neutral refractories are chemically stable at high temperatures against both basic and acidic environments. They are the most common preferred refractories because they can be used in both environments. However, neutral refractories are refractories with a chemical affinity at high temperatures. Neutral refractories that can operate at high temperatures and in aggressive environments are rare. Alumina (Al_2O_3), chromium oxide-chromia (Cr_2O_3), and graphite are examples of these refractories. For example, alumina and chromium oxide are chemically stable at low temperatures but exhibit acidic behavior at elevated temperatures and react with materials in basic environments.[20]

1.2.1.4. Special Refractories

Special refractory materials are narrower in the case of application areas than industrial refractories, but they are as important as industrial refractories. Here, we have separated the special refractory materials into oxides and non-oxide refractories.[20]

1.2.1.4.1. Oxide Based Refractories

Zircon-zirconia refractories are the leading oxide-based refractories. Zirconia (ZrO_2) is a chemically inert material with a high melting temperature. Zircon ($ZrSiO_4$) is a zirconium silicate material. Zircon has a wide range of applications due to its physical properties such as low thermal expansion coefficient, good thermal stability, and high corrosion resistance. Zirconia has refractory property over 2000˚C. It also has superior chemical resistance to acidic or basic environments. However, it cannot be used except for critical applications due to its high cost.[20]

1.2.1.4.2. Non-Oxide Refractories

Here, we separated the non-oxide refractory materials into carbides (SiC, B_4C, WC), nitrides (Si_3N, AlN, BN), and borides (TiB_2, ZrB_2). Some of the important properties of these refractories are shown in Table 1.1.

a. Carbides

SiC has properties such as high thermal conductivity, high strength and high resistance to thermal shock both at current conditions and at high temperatures. SiC is a lightweight (bulk density < 3 g.cm^{-3}) and very hard, abrasion-resistant material. Also, it has high oxidation resistance. Its thermal conductivity is 21 W (m.K)$^{-1}$ at 1000˚C. SiC is resistant to dilute acids and bases but decomposes in environments containing borax, basic carbonates, and cryolite.[20]

Boron carbide is a material with superior wear resistance and is the hardest material after diamond. It is also a material with high corrosion resistance, especially to the acids. Compared to the silicon carbide, the oxidation resistance is low. Since boron carbide has low fracture toughness, its applications are limited. Boron carbide is used as a metal antioxidant as a refractory material.[20]

Tungsten carbide ceramics, that act as metals, are also called cermet. They are highly wear-resistant materials. Which is why they are widely used in cutting tools, armors and abrasive materials. Tungsten carbide also has very good mechanical and physical properties such as impact resistance, dimensional stability, and heat resistance.

Therefore, they are used in critical applications requiring wear and abrasion resistance in refractories.[20]

Table 1.1. Some of the properties of non-oxide refractories.[20-24]

Material	Density (g.cm^{-3})	Melting Point (˚C)	Thermal Expansion Coefficient (10^{-6}°C^{-1})	Thermal Conductivity (W.m^{-1}.K^{-1})
SiC	3.21	2567	5.0	> 270
B$_4$C	2.52	2350	4.5	0.3
WC	15.5	2720	3.8	0.07
Si$_3$N$_4$	3.18	1900	3.3	22
AlN	3.25	2200	5	125
BN	2.27	3000	0.7	35
TiB$_2$	4.50	3225	8.1	60-120
ZrB$_2$	6.08	3250	6.9	45-135

b. Nitrides

Silicon nitride is also a compound with strong covalent bond properties like silicon carbide. It is a material with high wear and corrosion resistance. It also is a material with high thermal shock resistance property. Therefore, it is used in high-temperature applications such as hydrogen-oxygen rocket engines.[20]

Aluminum nitride is slowly devastated by mineral acids and strong bases and slowly hydrolyzed in water. On the other hand, it is very stable in inert atmospheres. aluminum nitride has quite good physical properties; such as low thermal expansion, high thermal conductivity, and low electrical conductivity.Examples of its main uses are substrates for electronic devices, heat sinks, and molten metal processing components.[20]

Although many types of boron nitride are present, almost all have a superior high-temperature (> 2500˚C) in inert atmospheres, but oxidize above 800 ºC in a normal air atmosphere. Although boron nitride has poor mechanical properties, its composites have superior thermal shock resistance and corrosion resistance. Generally, it is used as a high-

temperature insulation material.For example, it is used in plasma arc insulation and nuclear applications.[20]

c. Borides

Both borides (TiB_2 and ZrB_2) have a high melting temperature, hardness, low electrical resistance, thermal conductivity, and excellent corrosion resistance up to 1100 ° C. Both borides are resistant to strong acids such as HCl and HF but are weak to alkali metal hydrates and can be decomposed in them. They are used as high-temperature refractories in non-oxidizing atmospheres (2000-3000 ˚C) and have an important role in this field. TiB_2 is used in metallurgical applications (especially in molten aluminum) and also used in crucibles and armors as reinforcement material. ZrB_2 is used in the metallurgical industry, as a protective tube for the continuous temperature measurement.[20]

1.2.2. Manufacturing Method

The production methods of refractories generally vary to achieve the desired properties, shapes and sizes. Wherein the production methods of refractories were classified as follows; pressed and sintered, fused cast, hand-molded and bonding.[20]

1.2.2.1. Pressed and Sintered (Fired)

Most of the refractories are produced by pressin and sintering, which is the traditional method. Particles in different sizes (different raw materials contained in the refractory composition) are first mixed, then pressed and fired to produce the desired shapes and sizes. Critical parameters in this method are pressing pressure and firing temperature. These parameters are fixed according to the composition and characteristics of the targeted refractory. The use of low pressure and temperature results in relatively porous (less dense) products and these products have also relatively lower strength.[20]

1.2.2.2. Fused Cast

Fused cast refractories are obtained by melting and mixing oxide powders over 2000ºC in an electric arc furnace and then casting into the mold. The casted melt is solidified by annealing to avoid the generation of strain. These refractories are treated with oxygen while in the molten state, to make the refractory components highly oxidized. Fused cast refractories have a dense and highly stable structure compared to conventional refractories. They have superior mechanical and chemical properties. For instance, due to their high heat resistance, they can withstand high surface loads.[20]

1.2.2.3. Hand-Molded

Hand-molding method is used to produce critical shape and dimensional refractories. Non-conventional, critical forms are also important for a variety of applications. In most applications, the pressing method provides great convenience, but it is not efficient in complex forms. The dimensions of the shape also limit the pressing process, so it is easy and simple to use the hand-molding method to achieve the desired shape and size before firing. Hand-molded parts use more water (about two or three times more) than parts produced by pressing. Therefore, the green body strength is also lower. For this reason, the transport and drying of these parts is relatively critical. Comperatively more porous structures are obtained since relatively more water content and less compression pressure are used to shape these products. Also because of the high shrinkage after firing, the mold dimensions have to be adjusted accordingly.[20]

1.2.2.4. Chemically Bonded

Most of the refractories are chemically bonded. Which means that a chemical difference from the chemical nature of the refractory components is used to form a secondary chemical bond between the particles to maintain their shape and size, strength and other properties. Processes requiring high temperatures, such as direct sintering, are necessary to strengthen the bonds between the refractory components. The addition of a second phase to the system may react and melt to form a bond between the refractory particles, but this could affect the high-temperature behavior of the refractory.[20]

1.2.2.5. Ceramic Fibers

Ceramic fibers are a class of insulation materials that can be manufactured in any desired shape (such as sheet or paper) and can be used in many fields of applications. Ceramic fibers spun (bulk fibers) prevent heat loss to a great extent and due to high heat efficiency, they provide ease of heating and cooling in the application area (e.g. in furnaces). They are economically advantageous thanks to their lightweight structure and good thermal insulation properties and are preferred in terms of energy efficiency in the industry thanks to their fast heating and cooling properties. One of their disadvantages is their expense compared to conventional refractories. Their mechanical strength is relatively low, shrinkage and spalling can occur at high temperatures. Subjected to degradation in the presence of a liquid phase such as slag, molten metal, and glass. The Figure 1.1 shows the forms of ceramic fibers used in refractory applications.[20]
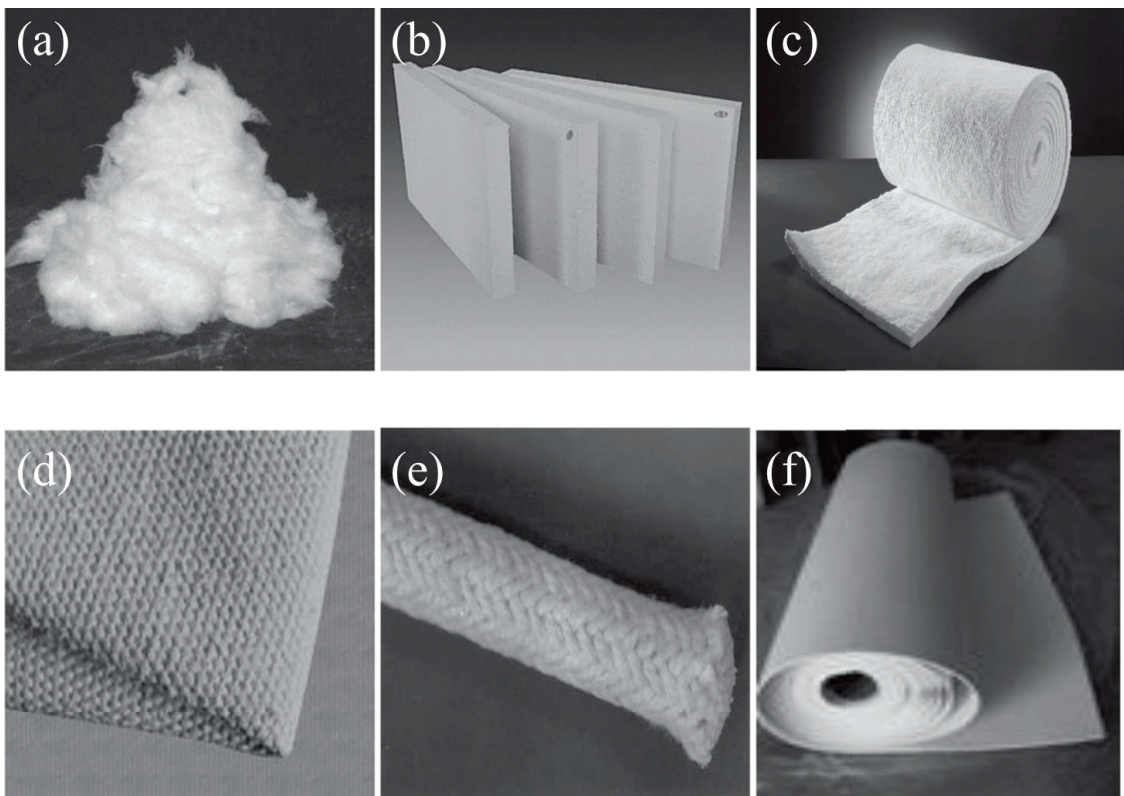
Figure 1.1. The ceramic fiber forms used in refractory applications; (a) bulk fiber, (b) board, (c) blanket, (d) cloth, (e) rope, and (f) paper (Source: Sarkar, 2016).[20]

While several compositions have been tested as thermal insulation, as detailed above, CS or CSHs materials have rarely been utilized as refractory in scientific studies.[25, 26]

1.3. The CSHs: Tobermorite and Xonotlite

The phase diagram of the system of CaO-SiO_2-H_2O stability under hydrothermal conditions is given in Figure 1.2. The production methods of these phases and general information about will be discussed in details. However, among all calcium silicate hydrates (CSHs), ones with calcium to silicon mole ratio $\leq$ 1, i.e. xonotlite $Ca_6Si_6O_{17}(OH)_2$ and tobermorite $Ca_5Si_6O_{16}(OH)_2 \cdot 4H_2O$ are the most studied ones.[27]
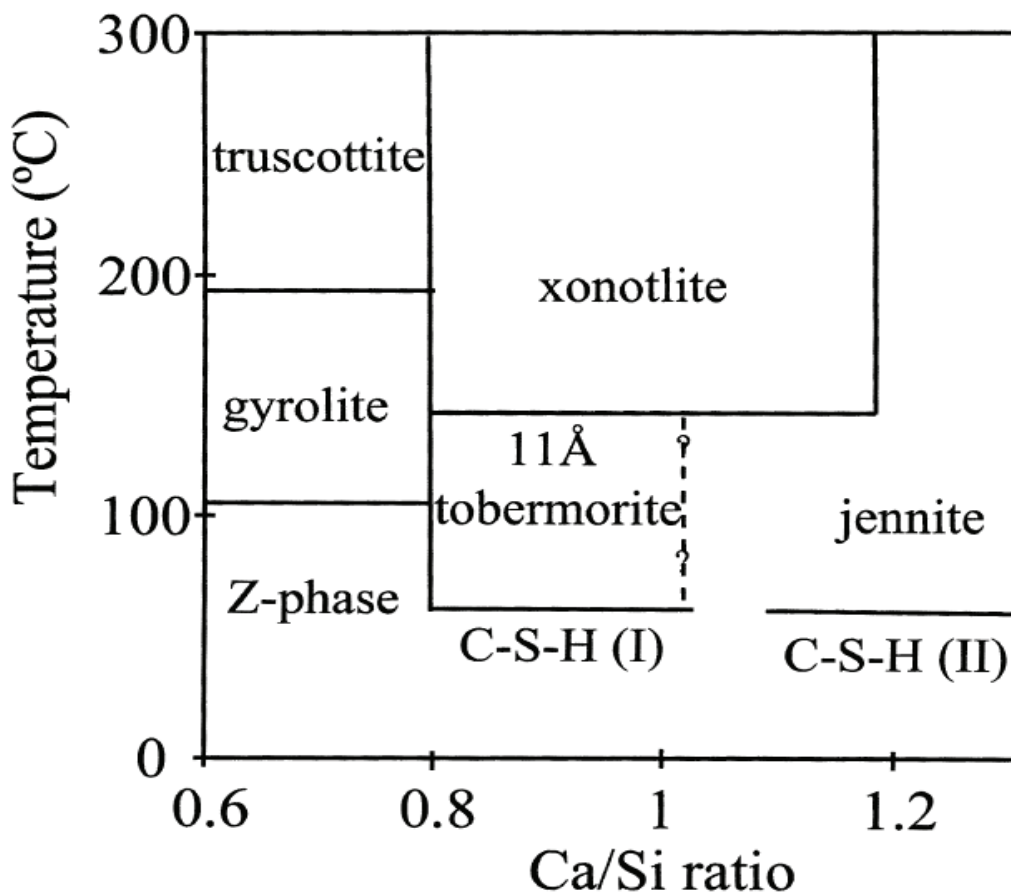
Figure 1.2. The effect of Ca/Si ratio and temperature variables on the CSH phases (Source: Shaw, 2000).[27]

1.3.1. Tobermorite

The name Tobermorite was came from Tobermory, Island of Mull (Scotland) where it was first discovered in 1880.[28] Despite the varying stoichiometry of its polymorphs, its general formula is shown as $Ca_5Si_6O_{16}(OH)_2 \cdot 4H_2O$.[29] Tobermorite has three separate polymorphs, named as 9, 11 and 14 Å tobermorite. This denomination indicates the d-distance of the (002) plane of the Bragg peaks,[27] as well as the amount of water contained in the tobermorite structure.[27, 30] Among these three polymorphs, 11 Å tobermorite is the most common in environmental conditions. 11 Å Tobermorite is categorized into "normal" and "anomalous" according to its dehydration behavior. If it can be transformed into 9 Å tobermorite at about 300˚C called normal, if it cannot be transformed, called as anomalous tobermorite.[31] 11 Å Tobermorite structure consists of an octahedra calcium layer; there is also a tetrahedra silicate chain on each side with a calcium layer in the center.[27, 30] The general morphology of the tobermorite phase is in the form of fibers and plates.[32] The SEM images of platelet and fibrous tobermorite are given in Figure 1.3.
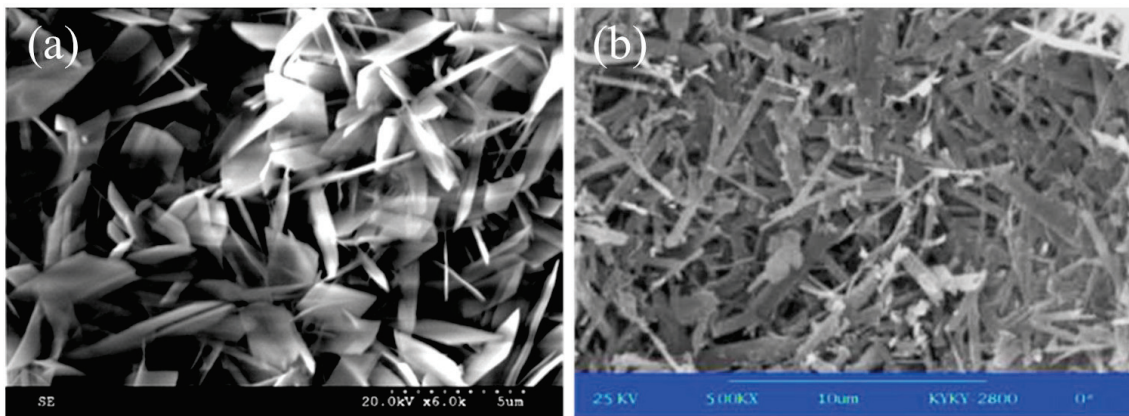
Figure 1.3. The SEM images of (a) platelet tobermorite and (b) the fibrous tobermorite (Sources: Mostafa, 2009 ; Yang, 2015).[33, 34]

Physical properties of tobermorite, the measured density is 2.423-2.458 $g.cm^{-3}$ and the calculated density is 2.49 $g.cm^{-3}$. Tobermorite have pinky white or white color and have a radiance like glassy. The optical property of tobermorite can be translucent or

transparent. There is no absolute precision about the hardness of tobermorite.[29] The molecular weight of tobermorite can be measured from the formula of $Ca_5Si_6O_{16}(OH)_2 \cdot 4H_2O$ as 730 g.mol^{-1}.

In the structure of the tobermorite, elements such as Al, Fe, Na, K can be substitute.[31] Al is the most substituted element. In the literature, it is obvious that the substitution of this element in the structure instead of Si^{4+}, is more common than the other elements, see.[2, 3, 7, 33-41] Not only the Al metal, but also the Co and Ni metals are replaced to the tobermorite structure, however instead of Ca metal.[42]

The usage of tobermorite is wide-ranging. For the most part, it is used as a binder material in cement systems providing high strength and improved microstructures.[32, 39, 43] Also used as decontaminating material for disposing the heavy metal ions from hazardous wastes.[2, 41, 44-48] Tobermorite is also used as an accelerator in the organic synthesis process[49] and adsorbent for carbon dioxide gas.[40]

1.3.2. Xonotlite

Xonotlite takes its name from the region was discovered in 1866 in Tetela de Xonotla, Mexico.[13, 50] The chemical formula of xonotlite is $Ca_6Si_6O_{17}(OH)_2$.[13, 29, 51] Xonotlite shows affinity with some minerals such as tobermorite, wollastonite $CaSiO_3$, diopside $CaMgSi_2O_6$ and thaumasite $Ca_3Si(SO_4)(CO_3)(OH)_6 \cdot 12H_2O$.[29] Calcium to silicon mole ratio is ordinarily to be 1 or smaller than 1.[52] Xonotlite has a hardness value between 6 and 6,5 on the Mohs scale. Density of measured that 2.71-2.72 g.cm^{-3} and calculated density is 2.71 g.cm^{-3}. The optical property of xonotlite is translucent and have a chalky white or dull pink color. Also have a pearly radiance on the surface of it.[29] The molecular weight of xonotlite can be calculated from the formula of $Ca_6Si_6O_{17}(OH)_2$ as 714 g.mol^{-1}. Natural xonotlite can be contains a trace of Na, Fe and Mn elements in its structure.[13] The Si^{4+} in the xonotlite structure can be up to 5% substituted by Al^{3+} metal.[53] Almost all the Ca^{2+} metal can be substituted with Co^{2+} or Ni^{2+} elements,[42] however Ca^{2+} metal can also be partially substituted by Mg^{2+} metal.[54]

The morphology of the xonotlite is fibrous and generally be referred to as needle-like, acicular or nanobelt in the literature. The SEM and TEM images of that morphology of those forms of xonotlite are given in Figure 1.4.
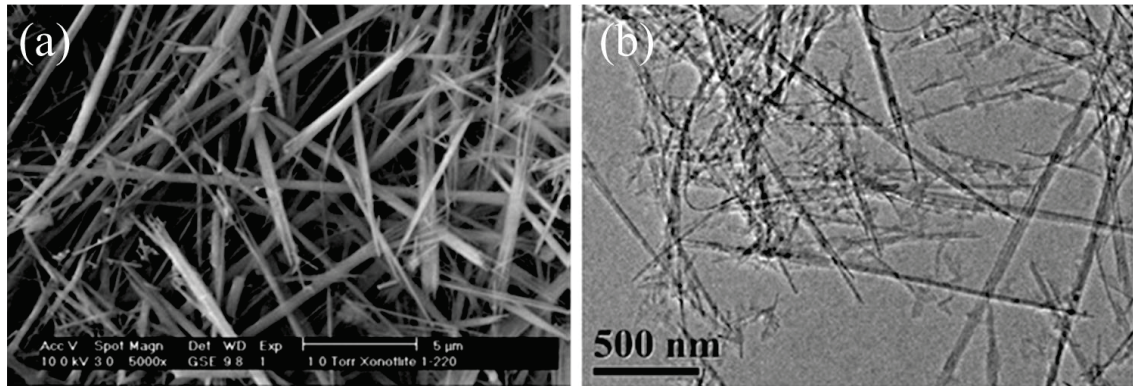
Figure 1.4. (a) The fibrous, and (b) nanobelt morphology of the xonotlite (Sources: Black, 2009 ; Wu, 2010).[13, 55]

Because of its special structure and various features, xonotlite is seen in many applications. For example, in brake linings, because of the increased operating temperatures during the friction, xonotlite is used as filling material due to its resistance to high temperatures.[56] Again because of the fire resistance property (high degree stability even at high temperatures, up to 800 ˚C) xonotlite can be used as a fire-proof material.[53, 57-59] Also, xonotlite is a phase which improves the structural and mechanical properties of cement by joining to cement structure like tobermorite.[13, 52] Xonotlite is also a very light-weight material and is used as an insulation material.[25] Since xonotlite is used as thermal insulation material, the thermal conductivity coefficient (k) is an important measure. Xonotlite bricks at a density of 128 $kg.m^{-3}$ synthesized using carbide slag have a thermal conductivity of 0.0416 $W.m^{-1}.K^{-1}$ at RT (297 K).[25] In another study, it was observed that this thermal conductivity value increased slightly as the temperature increased. A xonotlite brick with a density of 124.5 $kg.m^{-3}$ was k = 0.0416 $W.m^{-1}.K^{-1}$ at room temperature, which was 0.199 $W.m^{-1}.K^{-1}$ at 650˚C and above.[60] In addition, xonotlite and several other minerals in the cement structure can be used in the extraction and adsorption of Cs metal in the environment.[48]

1.4. Structure and Scope

The first chapter gave information about the introduction of this thesis. A comprehensive review of the literature given in chapter 2. This section includes information on tobermorite and xonotlite minerals and their production routes. The

experimental procedure of the study will be given in chapter 3. The results and the discussion about the study will be given in chapter 4. Finally, the conclusion of the study will be handled in chapter 5.

1.5. The Hydrothermal Synthesis

CSHs are mostly obtained by hydrothermal synthesis method. The term "hydrothermal" comes from earth sciences and was first used by a geologist to explain the effect of water under high temperature and pressure behavior on the formation of rocks and minerals.[61, 62] After understanding the formation of rocks and minerals in nature with the presence of water under high temperature and pressure, it has become popular by simulating these natural conditions to the laboratory environment. The first successful application in hydrothermal method was mineral extraction. Later applications were metalworking and inorganic compounds. Nowadays, hydrothermal synthesis has taken its place in many disciplines and combined with different techniques. Such as hydrothermal growth, hydrothermal decomposition, hydrothermal electrochemical reaction, hydrothermal dehydration, hydrothermal sintering, etc.[61]

The necessary parameters for the hydrothermal synthesis are temperature, (25 ˚C < T < 1000 ˚C) pressure (0.1 MPa < P <500 MPa) and aqueous media.[61, 63, 64] The necessary equipment is the autoclave, which provides these parameters and can withstand the elevated temperatures and pressures.[62] The given temperature and pressure ranges varies according to the temperature and pressure limits of the available autoclaves. In such closed systems, along with the temperature and pressure factor, the water occupancy rate also affects the system, see Figure1.5.

Considering the development of methods and equipment in hydrothermal synthesis, many of the first studies were carried out in gun barrels. Because the gun barrels were able to withstand high pressures, one of the required parameters. The closing of these gun barrels was provided by soldering or welding. In some cases, the cover gaskets were screwed. The disadvantage of such bombs is that they do not stand firm at high pressures and the pressure on the cover extends over a wide area and decreases the stress on the unit area. The next phase of bomb design was developed in terms of the closing mechanism. Thanks to the design, the pressure is applied to a small area and pressure loss is prevented from the walls of the bomb. Another type of bomb was developed by Morey

and Ingerson, although it was similar to the previous bomb as a closing mechanism, it provided higher pressure and resistance to temperatures as a design.[65]
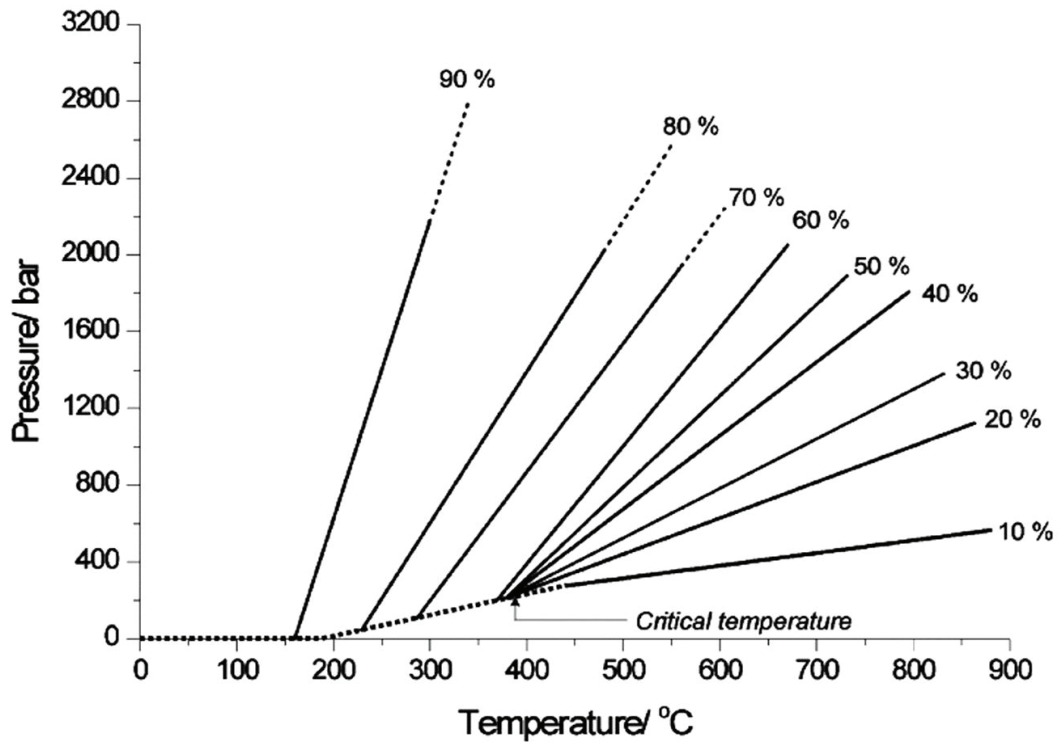
Figure 1.5. The effect of temperature and water occupancy rate on pressure in closed system (Source: Walton, 2002).[66]

CHAPTER 2

LITERATURE REVIEW

2.1. Production of Tobermorite and Xonotlite

Tobermorite and xonotlite, from CSHs family, are produced by hydrothermal synthesis. Tobermorite and xonotlite are defined as magmatic rocks[35, 52, 67, 68] and occur in the high basic conditions (hyper-alkaline), where hydrothermal conditions are achieved.[52, 69] In the process of tobermorite and xonotlite production, the important parameters affecting the production process are the starting materials (raw materials), water to solid ratio (W/S), temperature (T), time (t), Ca to Si molar ratio (Ca/Si) and also pH levels. In consequence of changing of these parameters, differences are observed in the properties of the final product, see.[34, 70-72] Factors such as the purity of calcium and silicon sources, the particle size and the impurities of the structure play an important role in the production process.[2] Also, the type of mixture preparation (pretreatments before the hydrothermal synthesis; mixing with ball mill etc.) and the autoclave conditions (if it is equipped with stirrer or heater) also affect the production process and the product that is to be formed.

In scientific studies, SiO_2 (in a crystallized or amorphous form) is used as the source of silicon, and CaO (usually by calcining of calcium carbonate - $CaCO_3$) is used as the source of calcium, for the synthesis of CSHs. In the classification of different parameters, when we look more closely to the starting materials, there are many studies that used SiO_2 and CaO as precursors.[5, 71, 73-77] Apart from these sources, there are also publications that used materials such as blast furnace slag,[2] K-feldspar,[34] borosilicate glass,[70] carbide slag,[25] clay bricks,[36] soda-lime-silica glass[43] or $Na_2SiO_3.9H_2O$ and $Ca(NO_3)_2 \cdot 4H_2O$ [55] as initiators. The parameter of W/S ratio in the literature was ranged from 1.00 [78] to 115.00 [37], the temperature ranged 60 $°C$ [79] up to 400 $°C$ [80] and the time ranged from 2h [81] up to 196 days.[82] When we look closely to the some synthesize productions;

CaO and SiO_2 were placed in the autoclave in the experiment that using silica fume (98% SiO_2) and limestone ($CaCO_3$) as starting material. In the case where the W/S ratio was low, the tobermorite and xonotlite phase existed as a mixture in the structure, while the W/S ratio (W/S=15) and the reaction time was higher (4h), highly crystalline xonotlite occurred in the system.[77]

In the study, two different hydrothermal reactions were performed using SiO_2 and $CaCO_3$ as the starting material and the temperature was 180˚C or 230˚C. In the experiments carried out at 180˚C, the Ca/Si molar ratio increased from 0.83 to 1.66 and the calcite and portlandite phase amounts increased in the structure. In the experiments where the temperature was 230˚C, the same parameters were changed with the experiments at 180ºC, at the end of the reactions xonotlite and hillebrandite $Ca_2SiO_3(OH)_2$ phases were observed in the structure.[74]

In the process of obtained tobermorite and then converted this tobermorite phase to zeolite P2 crystal, hydrothermal synthesis was performed in the autoclave using CaO and SiO_2 as starting materials. At the end of the hydrothermal process, they obtained tobermorite and then used this tobermorite phase in addition with the required chemicals to obtain zeolite crystal.[75]

2.1.1. Effects of Additives on the Production Routes

There are many studies about the effects of additives on the production routes in the literature. For instance, in the study that analyzing the phases and properties obtained products after the hydrothermal synthesis, as a starting material $Ca(OH)_2$ and SiO_2, and as an additive magnesite $Mg(OH)_2$ are used. Without additive, when only $Ca(OH)_2$ and SiO_2 are used, in both W/S ratio (0.64 and 0.90) xonotlite phase was observed in the final product. The addition of $Mg(OH)_2$ to the starting materials resulted in the formation of $4CaO.2MgO.6SiO_2.H_2O$ (unspecified structure).[71]

In a different study, CaO with SiO_2 as starting materials, sucrose ($C_{11}H_{22}O_{12}$), calcium formate $Ca(HCOO)_2$ and $CaCl_2.2H_2O$ were used as additive materials. In the ongoing reaction with SiO_2 and CaO, a high proportion of xonotlite (80% by weight), tobermorite and some unreacted quartz (2-3% by weight) were obtained. Although Ca/Si ratio was similar, in experiments using $CaCl_2.2H_2O$ as additive material, a smaller amount of xonotlite (51%, 56% by weight, respectively) were obtained compared to the

experiments using calcium formate $Ca(HCOO)_2$. In the experiment which added sucrose (Ca/Si = 0.56), the final product was calcite, quartz and scawtite $Ca_7Si_6O_{18}(CO_3)\cdot2H_2O$ phase.[73]

In another study that hydrothermal synthesis was performed using calcium silicate alkoxide and saturated $Ca(OH)_2$ solution. Al content in calcium silicate alkoxide has changed between 0% and 15%. According to the kinetical analyzes, it was observed that the increased Al content and increasing temperature lead to increase in reaction rate. At the increasing Al content and at low temperatures, the tobermorite phase is more stable in the structure, while at the low-Al content and at the high-temperature xonotlite phase are more stable in the structure.[27]

2.1.2. Production with Recycled Materials

Blast furnace slag (containing 33.75% SiO_2, 44.54% CaO, 8.16% Al_2O_3 and 10.39% MgO) and quartz (purity 99.9% SiO_2) used as a precursor in the study that carried out with the dynamic and static hydrothermal synthesis. In the experiment, which used only blast furnace slag with static hydrothermal synthesis, hydrogarnet and tobermorite were obtained. They observed that when the Ca/(Al+Si) mole ratio increased and adding rotation motion in the system, tobermorite phase formation was increased.[2]

In another study, conventional and microwave-assisted hydrothermal synthesis performed using similar raw materials above. $Ca(OH)_2$ and SiO_2, silicic acid (H_4SiO_4), borosilicate glass (mass content: 81% SiO_2, 13% B_2O_3, 4% Na_2O, 2% Al_2O_3 and 0.04% Fe_2O_3) were used as raw materials. In this study, the main difference between two parameters (except for the different silica sources and additives), was time; the time for conventional hydrothermal synthesis was 7 days, the reaction time for microwave-assisted synthesis was 8h. In both methods, tobermorite was obtained.[70]

According to the silicon source used in the experiments that different products were obtained, CaO, mullite ($3Al_2O_3\cdot2SiO_2$), colloidal silica (SiO_2) and clay bricks (%69,7 SiO_2, %18,6 Al_2O_3 containing.) were used as precursors. In a small amount of crystal form of 11 Å tobermorite were obtained from colloidal silica and CaO mixture. There was no change in the amount of crystalline tobermorite when mullite and clay brick added to the mixture, but the amount of tobermorite increased as the ratio of clay brick in

the mixture increased. At the end of the process, the tobermorite phase as well as the Al-substituted tobermorite phase were obtained.[36]

Besides, many studies have been examined and summarized in table. Table 2.1. summarizes the production conditions of some CS and CSHs in the literature.

Table 2.1. Synthesize process and obtained products of porous C-S-H's in literature.

Ingredients	Methodology	Process Conditions	Produced material(s)	Ref.
CaO, Silica Fume(SiO_2), $BaCl_2$	Hydrothermal treatment.	Ca/Si = 2 and W/S = 5, T = 110, 150˚C, t = 2 and 5h,	Hillebrandite $Ca_2(SiO_3)(OH)_2$	83
	Calcination of Hillebrandite.	600˚C-700˚C for 3h.	(Belite) β-C_2S powders	
CaO (from $CaCO_3$) or $Ca(OH)_2$, SiO_2 and NaOH	Hydrothermal treatment.	Ca/Si = 2, W/S = 10, T = 200˚C, t = 18h, 162h,22h	α-C_2SH	84
CaO (from $CaCO_3$), Silicic Acid (H_4SiO_4)	Hydrothermal Treatment.	Ca/Si = 2, W/S =20, T=200˚C, t= 2-3-5-10h & 10days.	α-C_2SH	85
Na_2SiO_3·$9H_2O$, NaOH, $Ca(NO_3)_2$·$4H_2O$	Hydrothermal Method.	T = 200˚C for 24 h.	$Ca_2(SiO_3)(OH)_2$ microbelts	86
$Ca_2(SiO_3)(OH)_2$ microbelts	Microwave	T = 670˚C for 2h	β-Ca_2SiO_4 microbelts (powder form)	

Table 2.1 (cont.)

CaO (from $CaCO_3$) Silicic Acid (H_4SiO_4)	Calcination of $CaCO_3$	T= 1050˚C, t= 3h.	$Ca_6(Si_2O_7)(OH)_6$ [jaffeite: $C_3SH_{1.5}$]	87
	Hydrothermal Treatment	Ca/Si = 3.0 and W/S = 20 stirring:150 rpm, T= 270˚C for 14 days.		
CaO from $CaCO_3$ and MgO from $MgCO_3$	Calcination.	T= 1000˚C for 4h at saturated vapor pressure.	$Mg_3Si_2O_5(OH)_4$ (MSH) Xonotlite $Ca_6Si_6O_{17}(OH)_2$ Tobermorite $Ca_5Si_6O_{16}(OH)_2$	88
CaO, SiO_2, MgO	Hydrothermal treatment.	Ca/Si = 0.8 & 1.5, P= 1-10MPa t=10h-3days, T=180 - 300˚C		
$Ca(OH)_2$, SiO_2, NaOH, H_2O	Hydrothermal treatment.	Ca/Si =2, W/S = 2, T= 190˚C t=6h,	$Ca_6(Si_2O_7)(OH)_2$ - jaffeite, and α-$Ca_2(HSiO_4)(OH)$	89
CaO from $Ca(OH)_2$, fly ash and glass, Gypsum ($CaSO_4$· $2H_2O$)	Agitation of solids.	350 rpm, 92˚C at autoclave.	They only say 'Calcium Silicate'	90
TEOS- $Si(OC_2H_5)_4$, $Ca(NO_3)_2$·$4H_2O$, $Mg(NO_3)_2$·$6H_2O$	Sol gel Method; With different two processes.	Mixing ingredients in distilled water. Then drying of sols at 100˚C for 24h. After, samples stabilized at 600˚C for 1 h.	Ca_2SiO_4 crystalline phase in Calcium Silicate Glass.	91

Table 2.1 (cont.)

TEOS- $Si(OC_2H_5)_4$, $Ca(NO_3)_2 \cdot 4H_2O$, $Mg(NO_3)_2 \cdot 6H_2O$ $CaCl_2$ solution (10μm size of carbon powders, to alginate the calcium)	Coprecipitation Process.	At RT, 400 rpm for 2h. During precipitation pH value: 10.5-10.7 Then Calcination of dried powder (Diopside) at 700°C for 2h.	Porous $CaMgSi_2O_6$-Diopside microspheres.	92
CaO, K-feldspar (chemical composition of $KAlSi_3O_8$: 64.7% SiO_2, 18.4% Al_2O_3, 16.9 K_2O)	Hydrothermal synthesis	$Ca/(Si + Al) = 0.83$, $W/S = 20$, $T = 180$ to 250°C, $t = 4 - 8h.$, stirring rate = 400rpm	Tobermorite: $Ca_5Si_6O_{16}(OH)_2 \cdot 4 H_2O$ (crystalline tobermorite obtained at W/S =20, T=250°C and t=8h)	34
$Ca(OH)_2$, SiO_2, (H_4SiO_4), Pyrex glass (chemical composition; 81%SiO_2, 13%B_2O_3, 4%Na_2O, 2%Al_2O_3 and 0.04%Fe_2O_3), EDTA $(C_{10}H_{16}N_2O_8)$, KOH	Hydrothermal Synthesis (samples also rotated)	$Ca/Si = 0.36-1.78$, $T = 200°C$, $t = 7days$, $pH = 13$	11Å Tobermorite	70
$Ca(OH)_2$, SiO_2, Silicic Acid (H_4SiO_4), Pyrex glass	Microwave assisted hydrothermal synthesis	$Ca/Si = 0.36-0.83$, $T = 200°C$, $t = 8h$		

Table 2.1 (cont.)

CaO, SiO$_2$, Mullite (3Al$_2$O$_3$·2SiO$_2$), Clay Brick (chemical composition: 69.71% SiO$_2$, 18.64%Al$_2$O$_3$, 7.48% Fe$_2$O$_3$, 1.88%K$_2$O, 0.95%MgO, 0.84% TiO2, 0.44% Na$_2$O and 0.21% CaO)	Hydrothermal Synthesis	Ca/Si = 0.80, W/S = 10, T= 180˚C, t=8 h	Tobermorite, Al-substituted Tobermorite.	36
Calcsilicate alkoxide, Ca(OH)$_2$ (as a solution)	Hydrothermal synthesis	Ca/(Al+Si) =0.83, W/S = 5, T= 190-310˚C, t=3-5h. (Al content 0% -15%)	Tobermorite Ca$_5$Si$_6$O$_{16}$(OH)$_2$·4 H$_2$O and Xonotlite Ca$_6$Si$_6$O$_{17}$(OH)$_2$	27
SiO$_2$, CaO Additives:		Ca/Si = 0.8, T= 220˚C, t= 40.5h, W/S =7.5	Xonotlite (80% by wt.), 11 A Tobermorite (16% by wt.),	
Sucrose C$_{12}$H$_{22}$O$_{11}$	Hydrothermal synthesis	Ca/Si = 0.56	Scawtite C$_7$S$_6$H$_3$C calcite, quartz	73
Ca-Formate Ca(HCOO)$_2$		Ca/Si =0.8	Xonotlite (51% by wt.), Quartz, Calcite	
CaCl$_2$.2H$_2$O		Ca/Si =0.8	Xonotlite (56% by wt.) 11Å Tobermorite (30% by wt.)	

Table 2.1 (cont.)

Quartz(SiO_2) CaO (from $CaCO_3$)	Hydrothermal synthesis	Ca/Si = 0.41, 0.55, 0.83, 1.24, 1.66 T= 180& 230˚C, t=40.5 h, W/S = 7.5	11Å Tobermorite, Xonotlite Hillebrandite	74
CaO (from $CaCO_3$) SiO_2	Hydrothermal synthesis	Ca/Si = 0.83, W/S=10, T= 175˚C, t= 24 h	11Å Tobermorite (tobermorite used for zeolite production as a silica source).	75
$CaCO_3$ (99%) SiO_2 (99%)	Mechano-chemical method	Stirring rate= 300rpm, T= room temperature, Milling times:1-26h	Wollastonite $CaSiO_3$	76
Silica fume (98% SiO_2) CaO (from $CaCO_3$)	Hydrothermal synthesis (autoclave is equipped with Stirring)	W/S = 10 and 15, T=200˚C, t=2h and 4h, Stirring rate = 20 rpm	Xonotlite (high crystalline; at the conditions of C/S=1, W/S=15, T=200˚C, t=4h)	77
Ca(NO_3)$_2$·4H_2O Na_2SiO_3·9H_2O	Microwave assisted hydrothermal synthesis	Ca/Si = 2 (0.8, 1.0, 3.0 also), T=180˚C, t=90 min.	Xonotlite $Ca_6Si_6O_{17}(OH)_2$ nanobelts	55
		Xonotlite nanobelts transforms to wollastonite at 800˚C for 2h	Wollastonite β-$CaSiO_3$	
SiO_2 Ca(OH)$_2$ KOH	Hydrothermal synthesis	Ca/Si = 1,T= 220˚C, t= 15 h, Pressure (P) = 2.4 MPa, pH= 12-13.5	Xonotlite fibers	72

CHAPTER 3

EXPERIMENTAL

3.1. The Raw Materials

The calcium silicate hydrate powders were mainly synthesized from recycled glass (kindly provided from Şişecam Company, İstanbul, Turkey) and lime - $Ca(OH)_2$ (TS EN 459-1 CL 90S, provided from Nuh Kireç, Kocaeli, Turkey). The chemical compositions of the starting materials are given in the Table 3.1. The deionized water (Ultrapure Type-I, 18.2 MΩ.cm at 25˚C) was supplied by using a Millipak Direct-Q® 8 UV water purification system. The recycled glass was first crushed, then ground and sieved. The obtained recycled glass powder has a particle size of <25 µm.

Table 3.1. The chemical compositions of the recycled glass and lime.

Recycled Glass, RG (wt.% content)		Lime - $Ca(OH)_2$ (wt.% content)	
SiO_2	71.59%	Purity	90.41%
CaO	8.73%	MgO	Max. 3.00%
Al_2O_3	1.23%	SO_3	Max. 2.00%
MgO	4.17%	Free Water	Max. 1.00%
Na_2O	13.63%	Loss on Ignition	Max. 4.00%

Apart from the recycling glass, silica fume (Sigma, Aldrich, Silica - 99.8%) and quartz (supplied from Kale Ceramics, Çanakkale) were also used as a source of silica in the experimental procedure. Chemical composition information of quartz is also shown in Table 3.2. The purity of the silica fume (CAS Number: 112945-52-5) is 99.8%.

Table 3.2. The chemical composition of the quartz.

Quartz (wt.% content)	
SiO_2	98.93%
Al_2O_3	0.68%
TiO_2	0.05%
Fe_2O_3	0.01%
Na_2O	0.07%
CaO	0.02%
MgO	0.02%
K_2O	0.02%

3.2. Equipment

Retsch Planetary Ball Mill PM100 used for the mixing process. The grinding jar and balls type is agate (SiO_2) material. The agate grinding balls have a 13mm diameter.

Parr Industry, acid digestion vessel 4748A model static autoclave was used to perform the hydrothermal synthesis process. Prepared slurry was put into PTFE Teflon cup and reacted in autoclave. Their images are shown in the Figure 3.1. The reactor volume has a capacity of 125 ml. The working temperature of the reactor is up to 250˚C and the working pressure up to 13 MPa (131 bar) maximum.

3.3. The Powder Synthesis Procedure

$Ca(OH)_2$ was calcined at 1000˚C for 2 h (5˚C.min^{-1} heating rate) just in case and kept at in oven at 90˚C. Also, recycled glass kept at an oven at 90˚C continuously. For the starting of an experiment, $Ca(OH)_2$, recycled glass (or silica fume, quartz) and 20 ml of deionized water were added to the grinding jar and milled at 250 rpm for 10 h. After the milling process was completed, the slurry was transferred to the beaker from the agate jar. Deionized water was added to the milled slurry as so to the final volume of the new slurry 70 ml. The final slurry poured into the PTFE vessel. Before the hydrothermal reaction, the pH measurement of the slurry was made. Then PTFE vessel was placed into

the autoclave and sealed. The hydrothermal process was performed at the range of 160-220°C for 20-72 h. After the reaction completed, the autoclave opened and the pH measurement of the obtained products was made. The product obtained after the reaction was washed with DI water several times while the filtering process was made. Then the filtered product was dried at 90°C overnight.

Figure 3.1. The photographs of the used PTFE Teflon, the photograph and schematics of the autoclave[93] from left to the right respectively.

The Ca/Si mole ratio, which is one of the parameters affecting the process and the product obtained, was 0.83 and 1.00 in experiments using that recycled glass, quartz, and silica fume. Except for the Ca/Si mole ratio, the W/S ratio was 20, 25, 30 and 40 by weight, and the temperature parameter was 160,180, 200 and 220°C. The time parameter was also carried out as 20, 30, 50 and 72h. As a preliminary study or for observation purposes, some of the parameters specified in some experiments were exceeded. And at the same time, some parameters have not been tested with the assumption that they are not needed.

3.4. Analytical Methods

The morphological properties of the obtained products were analyzed by Scanning Electron Microscopy (SEM; Quanta 250, FEI, Hillsboro, OR, USA). The surface of the

samples was coated with a thickness of ~10 nm of Au. Phase analysis of the powders was analyzed with the Philips X'Pert Pro instrument (2θ, from 10˚ to 90˚and the scan step; 0.005 ˚/second). Decomposition behavior and phase transition points of the powders were analyzed by thermogravimetric analysis (TGA, Netzsch STA 409, Netzsch Gerätebau Gmbh, Selb, Germany). The samples were heated from RT to 1200˚C with a 5˚C. min^{-1} heating rate in air.

CHAPTER 4

RESULTS AND DISCUSSION

4.1. Microstructural Characterization of the Starting Materials

Microstructural analysis was conducted to the starting materials to investigate their shapes and phases. SEM images of the starting materials are shown in Figure 4.1.
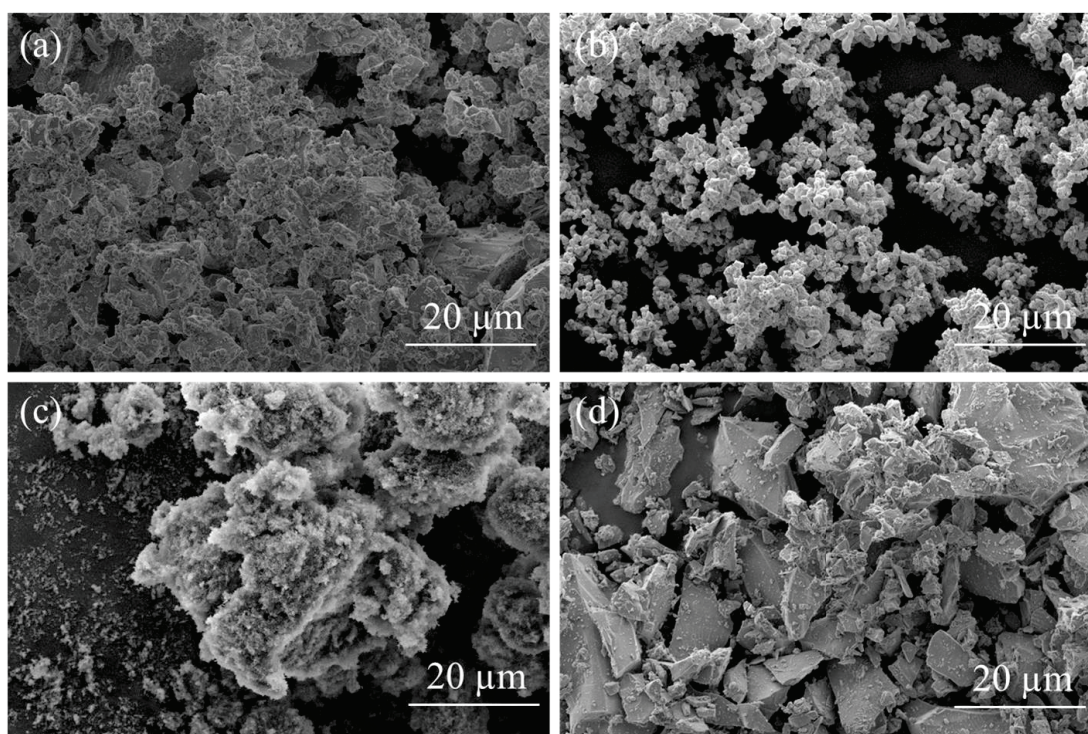

Figure 4.1. The SEM images of the starting materials, (a) recycled glass, (b) calcium hydroxide, (c) silica fume, (d) quartz.

The phase analysis was conducted with XRD, and the results are shown in Figure 4.2. According to the peaks obtained from the XRD analysis, the quartz peaks are

perfectly matched to the patterns of ICDD 46-1045, see Figure 4.2 (a). Calcinated form of calcium source was also analyzed by XRD analysis. According to the XRD result, the main phase of the non-heat treated calcium source is ICDD 44-1481 calcium hydroxide.

The phases of the heat-treated calcium source are the mixture of ICDD 44-1481 calcium hydroxide and ICDD 37-1497 calcia (CaO) as shown in Figure 4.2 (b).
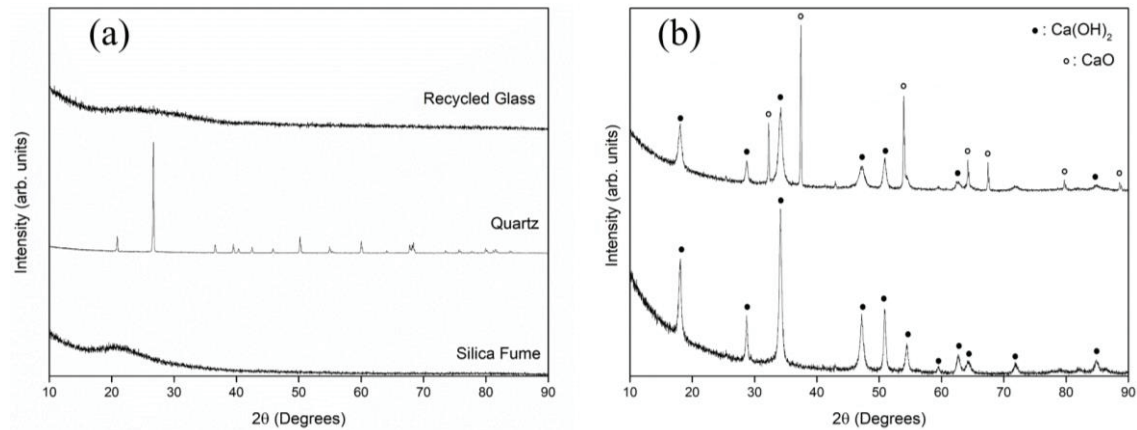
Figure 4.2. The XRD patterns of the starting materials (a) silica sources, (b) before (bottom) and after (top) calcination of calcium source.

4.2. Synthesis of CSHs with Different Silica Sources

The calcium silicate hydrate synthesis processes were carried out using different silica sources such as quartz, silica fume, and recycled glass.

4.2.1. Synthesis with Quartz

In the experiments that using quartz as the silica source, the test parameters were Ca/Si was 0.83 and 1.00, the W/S ratio was 20, 25, 30 and 40, t was 20, 50 and 72h, T = 160, 180, 200 and 220°C. In some parameters, the xonotlite phase or tobermorite-xonotlite phase was obtained, but this was not repeatable. In the obtained phases, residual quartz and calcite phases appear as the main peaks in the XRD analysis. This may be due to the relatively large particle size of the quartz and its inability to react sufficiently, leaving it as a residue in the structure.[79]

In the experiment with Ca/Si 0.83, W/S 20, t = 20h and T = 220˚C, ICDD No. 86-1629 quartz remained in the structure. The overall structure was analyzed as low-intensity ICDD No. 03-0241 tobermorite. In the experiment with Ca/Si 0.1.00, W/S 20, t = 20h and T = 220˚C, ICDD No. 86-2339 calcite remained in the structure. The overall structure was analyzed as low-intensity ICDD No. 19-1364 tobermorite. The obtained results are shown in Figure 4.3.
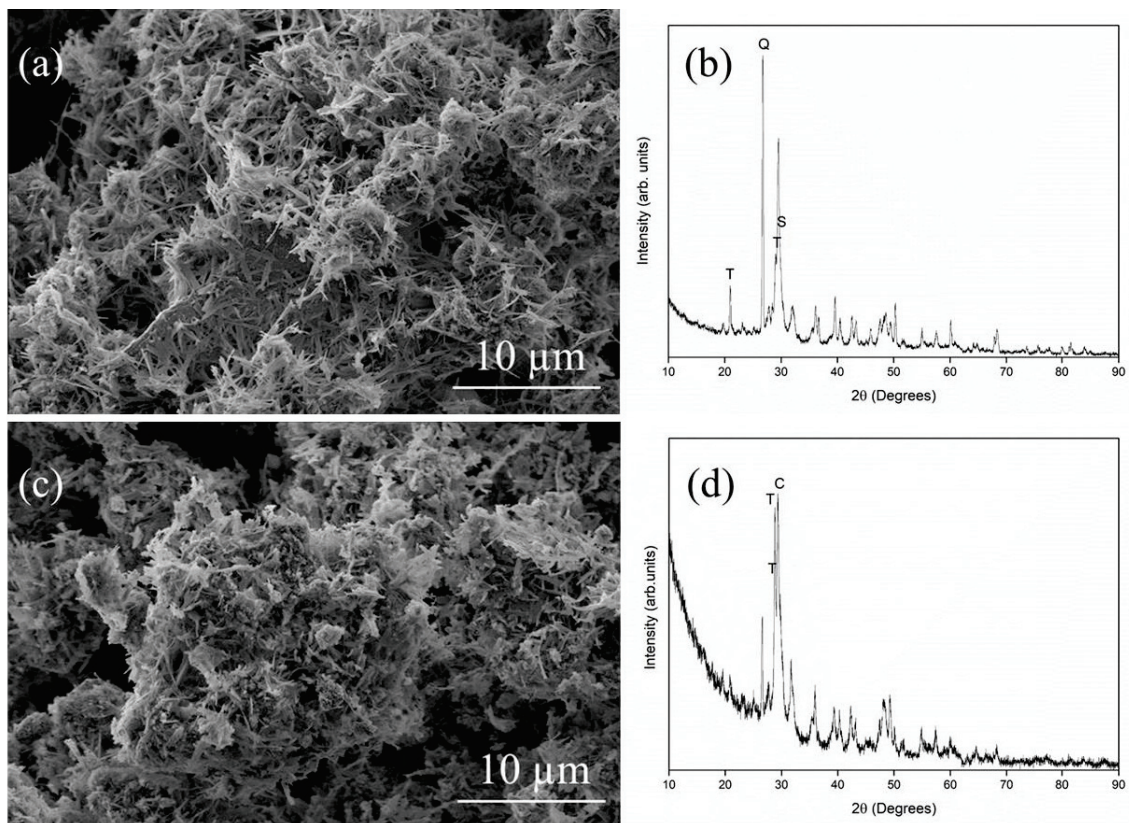
Figure 4.3. The SEM and XRD results of the experiments with the parameters of (a & b) Ca/Si=0.83, W/S=20, t=20h, T=220˚C, (c & d) Ca/Si=1.00, W/S=20, t=20h, T=220˚C (C: Calcite, Q: Quartz, S: Scawtite, T: Tobermorite).

4.2.2. Synthesis with Silica Fume

Concerning the quartz experiments, some parameters in the silica fume experiments were restricted. In this test set, experimental parameters were Ca/Si 0.83 and 1.00, W/S ratio 20 and 40, t=20h, and T=220˚C. As in the experiments with quartz, in the phases obtained using silica fume, the residual calcite and quartz remained in the

structure. XRD analysis of the product obtained with test parameters Ca/Si = 0.83, W/S = 20, t = 20h, and T = 220˚C was examined and ICDD No. 86-2334 calcite was observed at high intensity. The obtained phase was also partially compatible with the ICDD No. 70-1279 scawtite peaks, see Figure 4.4. It was observed that xonotlite or tobermorite could not be obtained with these experimental parameters.
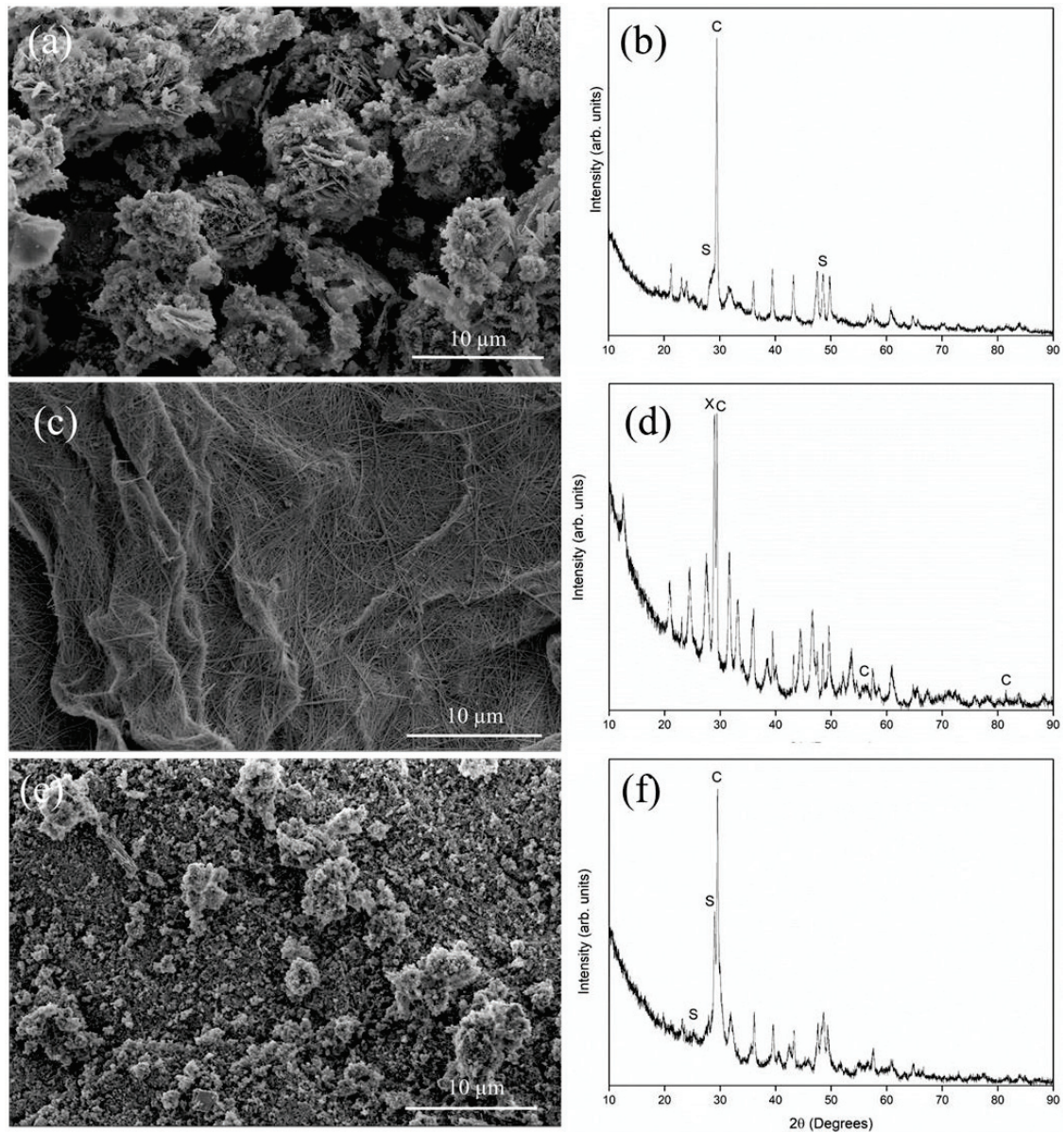

Figure 4.4. The SEM images and XRD analysis results of the aforementioned experiments, (a & b) Ca/Si=0.83, W/S=20, t=20h, T=220˚C, (c & d) Ca/Si=1.00, W/S=20, t=20h, T=220˚C, (e & f) repetitive experiment for the Ca/Si=1.00, W/S=20, t=20h, T=220˚C (C: Calcite, S: Scawtite, X: Xonotlite).

The xonotlite phase was obtained in the experiment with Ca/Si = 1, W/S ratio 20, T = 220˚C and t = 20h, but again, calcite remained as a residue in the structure. When the same test parameters were repeated, the xonotlite phase could not be obtained. According to XRD analysis, ICDD No 85-1108 calcite and ICDD No 70-1279 scawtite phase were observed in the structure, see the results in Figure 4.4.

As can be seen from the results gathered, the xonotlite or tobermorite phases could not be reproducibly synthesized using these silica sources. The main purpose of this thesis is to obtain the xonotlite phase by using more recyclable materials in relatively more economical ways. For these purposes, the emphasis was given to the experiments using recycling glass as the source of silica.

4.2.3. Synthesis with Recycled Glass

In light of the previous experiments with quartz and silica fume, the parameters of the experiments with recycled glass were fixed. The experiment parameters were tested such that the Ca/Si ratio was 0.83 and 1.00, the W/S ratio was 20 and 40, t = 20h and T = 160˚C or 220˚C. The time of the synthesis did not affect the morphology and crystallographic structure positively or negatively as observed from previous experiments. Therefore, according to the economic level, the time parameter was kept constant at 20 h. T = 160˚C experiments for W/S = 40 were not performed regarding the observations in the previous experiments. The experiments performed according to these parameters are shown in Table 4.1. SEM and XRD analysis result of the aforementioned experiments is shown in Figure 4.5.

Table 4.1. The table of the experiments performed, parameters and codes.

Sample Code	Ca/Si (mole ratio)	W/S (by weight)	t (h)	T (˚C)
CSH-1	0.83	20	20	220
CSH-2	1.00	20	20	220
CSH-3	0.83	20	20	160
CSH-4	1.00	20	20	160
CSH-5	0.83	40	20	220
CSH-6	1.00	40	20	220
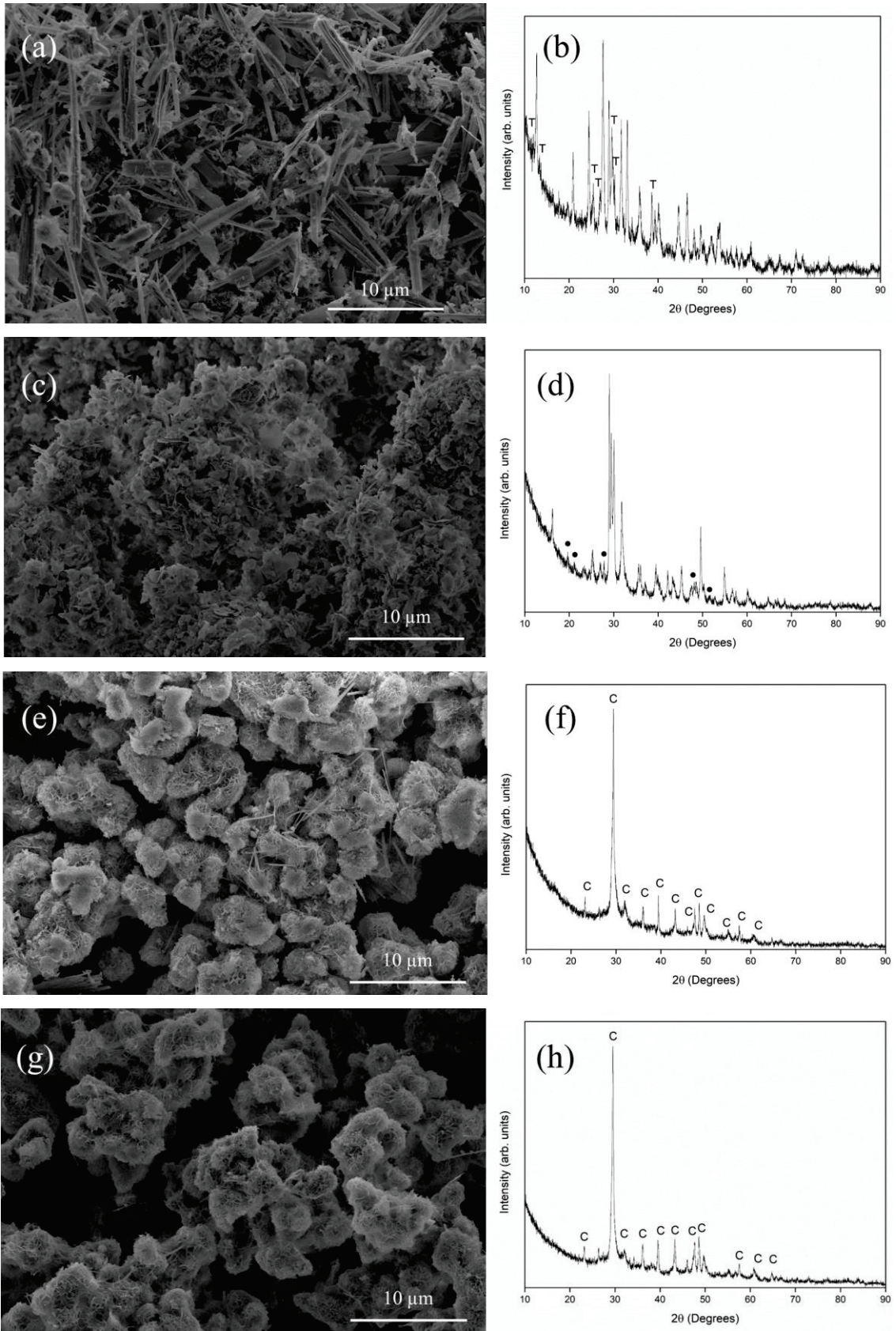
Figure 4.5. (Cont. on the next page)
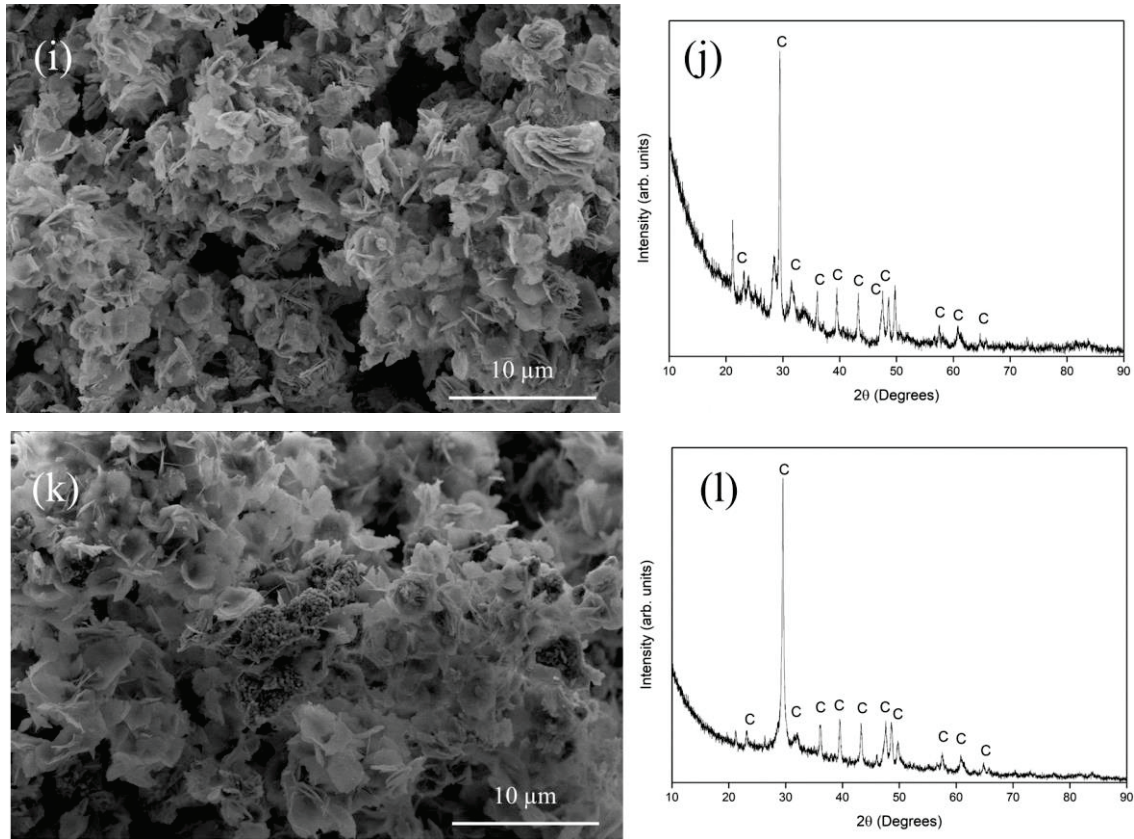
Figure 4.5. The SEM and XRD analysis results of the (a & b) CSH-1, (c & d) CSH-2, (e & f) CSH-3, (g & h) CSH-4, (i & j) CSH-5, and (k & l) CSH-6 respectively (C: Calcite, T: Tobermorite, ●: CSH phase). (cont.)

The main phase of the CSH-1 sample is ICDD 23-0125 xonotlite, but mismatched peaks are present. ICDD 29-0331 Tobermorite 14Å matches some peaks, shown in Figure 4.5 (b). The main phase of the CSH-2 sample is ICDD 19-1364 11Å tobermorite, but mismatched peaks are present. ICDD 03-0611 The Calcium silicate hydrate phase matches with some peaks, as shown in Figure 4.5 (d). The CSH-3 sample contains a high calcite phase. ICDD 81-2027 calcite has an intense peak that matched, it is shown in Figure 4.5 (f). The CSH-4 sample also contains a high proportion of calcium carbonate phase. The ICDD 85-1108 calcium carbonate phase is in agreement with the intense peak, as shown in Figure 4.5 (h). The CSH-5 sample matches the ICDD 72-1214 synthetic calcite phase, but there are mismatched peaks. The unmatched peaks also do not match any of tobermorite or xonotlite phases. The results shown in Figure 4.5 (j). The CSH-6 sample like CSH-5 sample matches the ICDD 85-1108 calcite, but there are mismatched peaks. The unmatched peaks also do not fit the any of tobermorite or xonotlite phases. The results are shown in Figure 4.5 (l).

According to the results gathered, the best xonotlite phase test parameters were obtained with Ca/Si = 0.83, W/S = 20, t = 20h and T = 220˚C. At high temperatures (>150 ˚C), it is possible to obtain the xonotlite phase with Ca/Si = 0.83, see xonotlite region on the Figure 1.2.[27] Sample with the best results CSH-1, to test the reproducibility of the sample, repetitive experiments were performed from the same sample. Almost thirty repetitive experiments yielded the same main phase ICDD 23-0125 xonotlite. A new batch was formed with powders from about thirty separate experiments. XRD, SEM, and TG-DTA tests were also applied to this obtained batch. This batch is called CSH.

4.3. Characterization Results of the CSH Sample

The SEM images of the CSH sample are shown in Figure 4.6. As seen from the SEM images of the CSH sample, the overall morphology is mainly fibrous and homogeneously distributed, but in some parts, lump structures are observed in high magnifications in Figure 4.6. (f, g & h).

The XRD analysis results of the CSH sample is shown in Figure 4.7. and the quantitative results shown in Table 4.2. The XRD quantitative analysis was performed using the Maud software by the Rietveld method.[94, 95] According to the quantitative analysis obtained, the CSH sample was contained 60.73% xonotlite (ICDD No. 23-0125), 9.81% tobermorite (ICDD No. 86-2275), 17.84% scawtite (ICDD No. 70-1279) as main phases. The average crystal size was determined using the analytical isotropic size model.[96, 97] Except for the main phase of xonotlite, other phases show values of around 1000 Å, while xonotlite has a value of 500 Å, which could be seen from SEM images (Figure 4.6) of the CSH sample. As can be seen from the XRD results, it is possible to produce high incidence of xonotlite and calcium silicate hydrates phase using recycled glass.

The CSH sample was also thermally analyzed as shown in Figure 4.8. According to the TG curve (black-dashed), the CSH sample was lost less than 20% of its total weight. This weight loss is reached at 817˚C and continued in the same level till to the final temperature of the analysis 1200˚C, i.e. above 817˚C temperature there is almost no weight loss. This stability at high temperature can be due to the conversion of CSHs to wollastonite.[98]
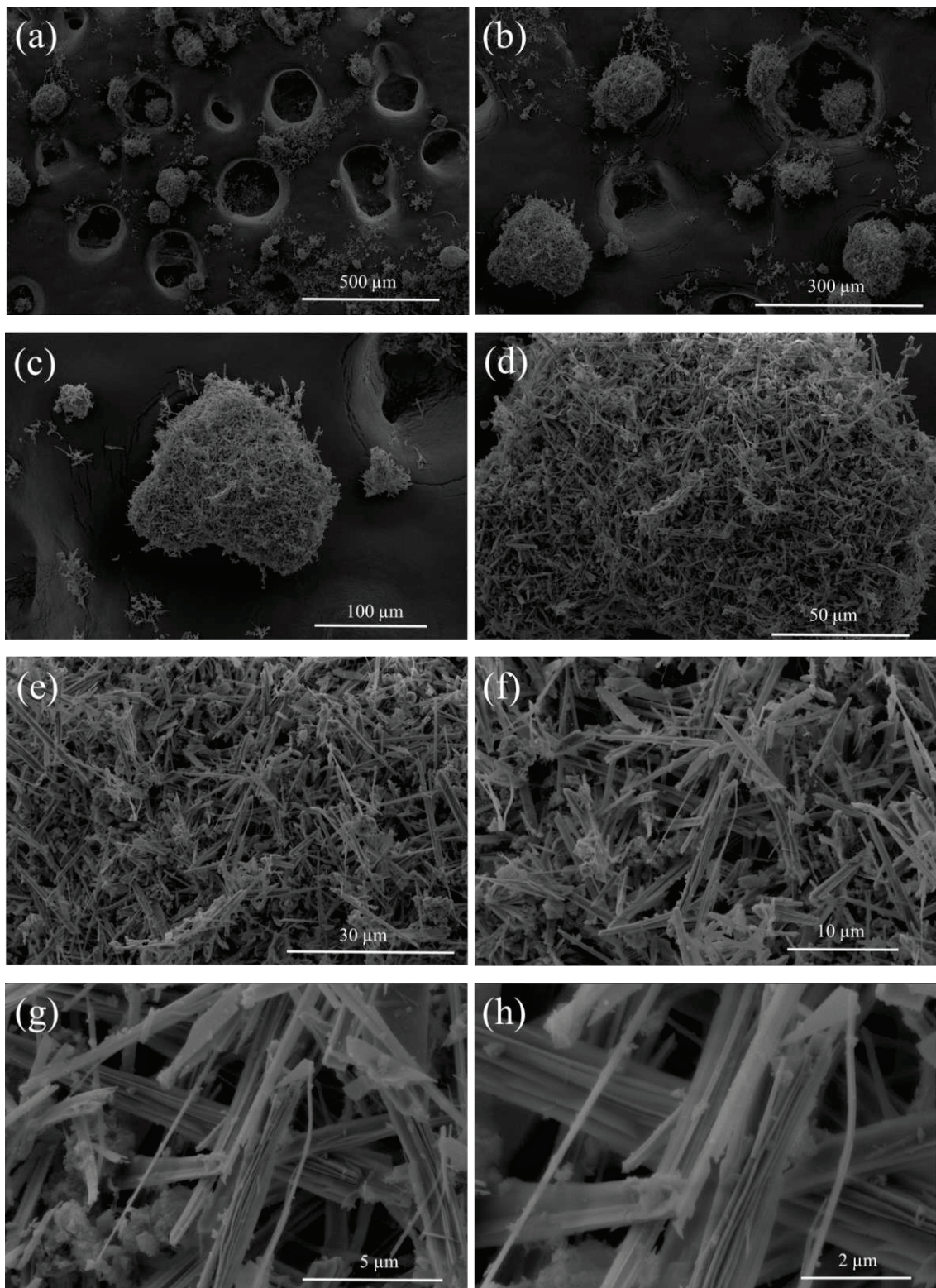
Figure 4.6. SEM results of the CSH sample. Magnifications are increasing from (a) to (h). The large holes in (a) and (b) refer to carbon tape.
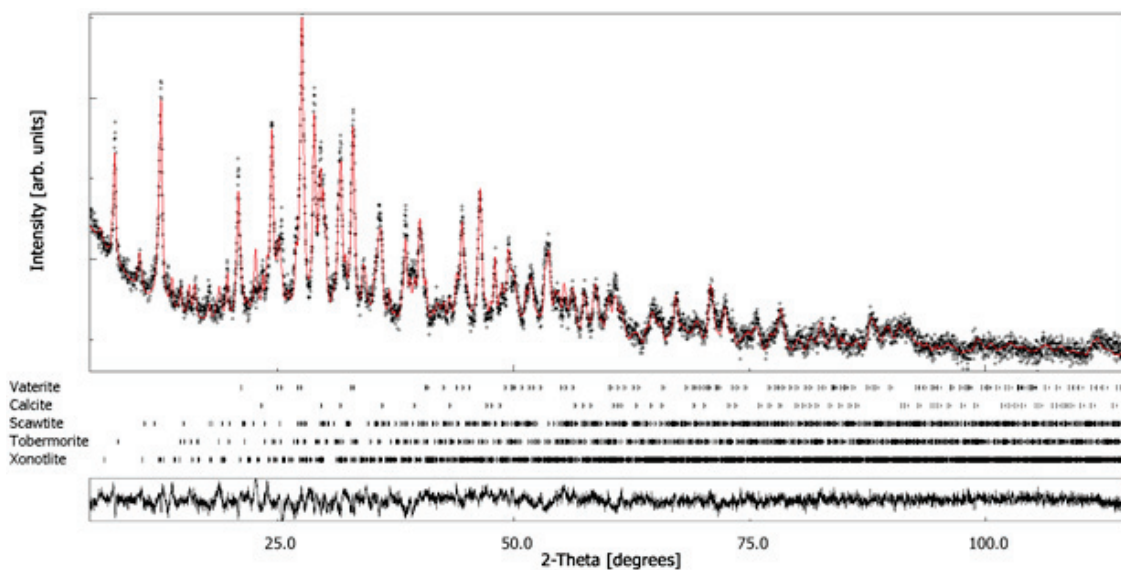
Figure 4.7. The XRD pattern and Rietveld fit of diffraction data collected from the hydrothermally synthesized CSH sample (The red lines are the main XRD pattern of the CSH samples, the black dots are the references for candidate phases).

Table 4.2. The quantitative content of the phases on the CSH sample and average crystallite size as obtained from the Rietveld fitting.

Phase	Formula	Weight (%)	Average Crystallite size (Å)
Xonotlite	$Ca_6Si_6O_{17}(OH)_2$	60.73	532
Tobermorite	$Ca_5Si_6O_{16}(OH)_2 \cdot 4(H_2O)$	9.81	1152
Scawtite	$Ca_7Si_6O_{18}CO_3 \cdot 2(H_2O)$	17.84	908
Calcite	$CaCO_3$	2.58	1022
Vaterite	$CaCO_3$	9.04	927

It was previously shown in the literature that if the system was pure xonotlite, no exothermic peak appears on the DTA data above around 800 ˚C because xonotlite was shown to have a topotactic transition, i.e., the topotactic transition means that the initial structure suits the final structure in three dimensions during the reaction.[53, 99] However, if the system is not constituted merely by xonotlite but also by other CSHs such as tobermorite, it demonstrates an exothermic peak at about 810˚C, as shown previously by

other studies.[77, 100] Since the DTA curve given in Figure 4.8. shows an exothermic peak at about 805˚C, it is possible to comment that the CSH powder synthesized by the current study includes mixed CSHs, i.e. not pure xonotlite. It is important to note also that such exothermic peak indicates the formation of wollastonite phase similar to other works.[100]
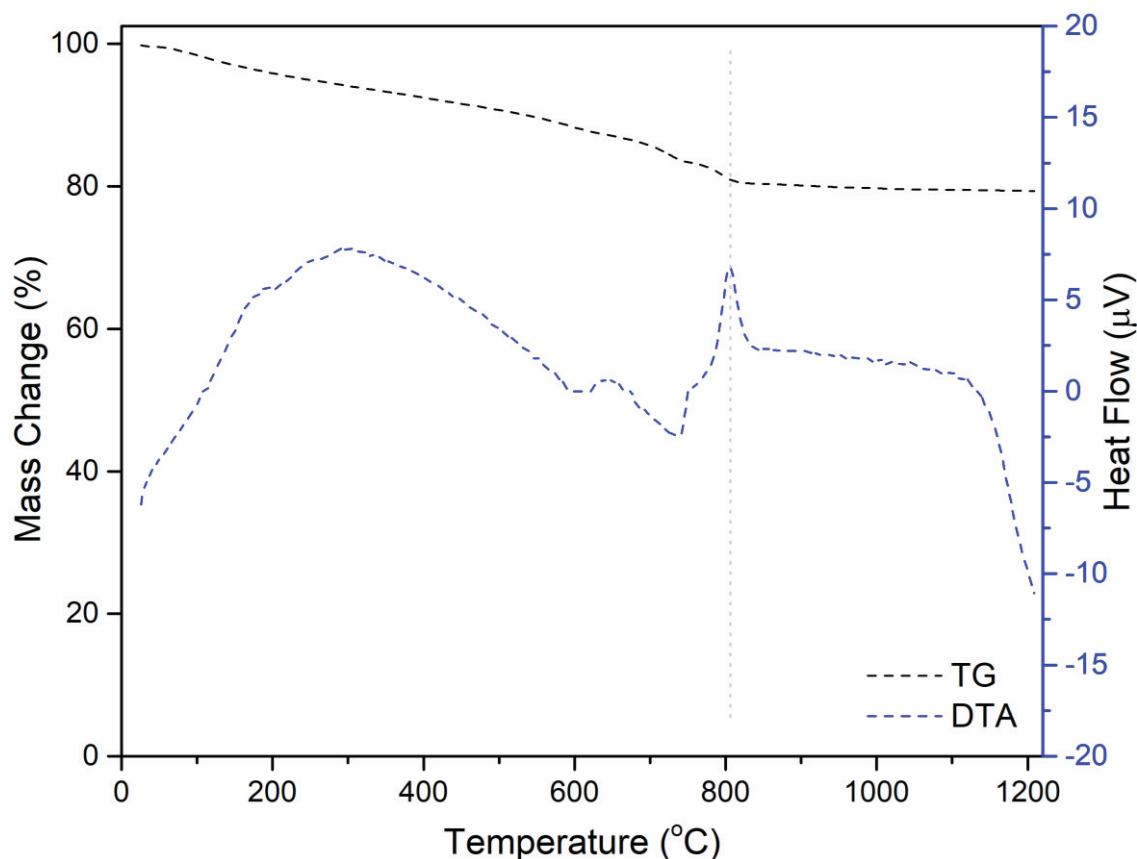
Figure 4.8. The TG-DTA analysis result of the CSH sample. The dotted vertical line at 800˚C demonstrates the exothermic peak.

TG/DTA was also applied to the calcined powder (1000˚C for 2 h), during which CSH transformed into wollastonite, see Figure 4.9.[77] It is clear that the formed material is highly stable to heating, see a very low weight loss (below 1%) up to 1200˚C. The slight endothermic peak forming at around 1135˚C may be attributed to the initiation of the decomposition of the system,[25] since previously it was shown that β-wollastonite is stable up to 1250˚C. In this previous study, above the 1250˚C β-wollastonite has transformed into the α-wollastonite.[101]
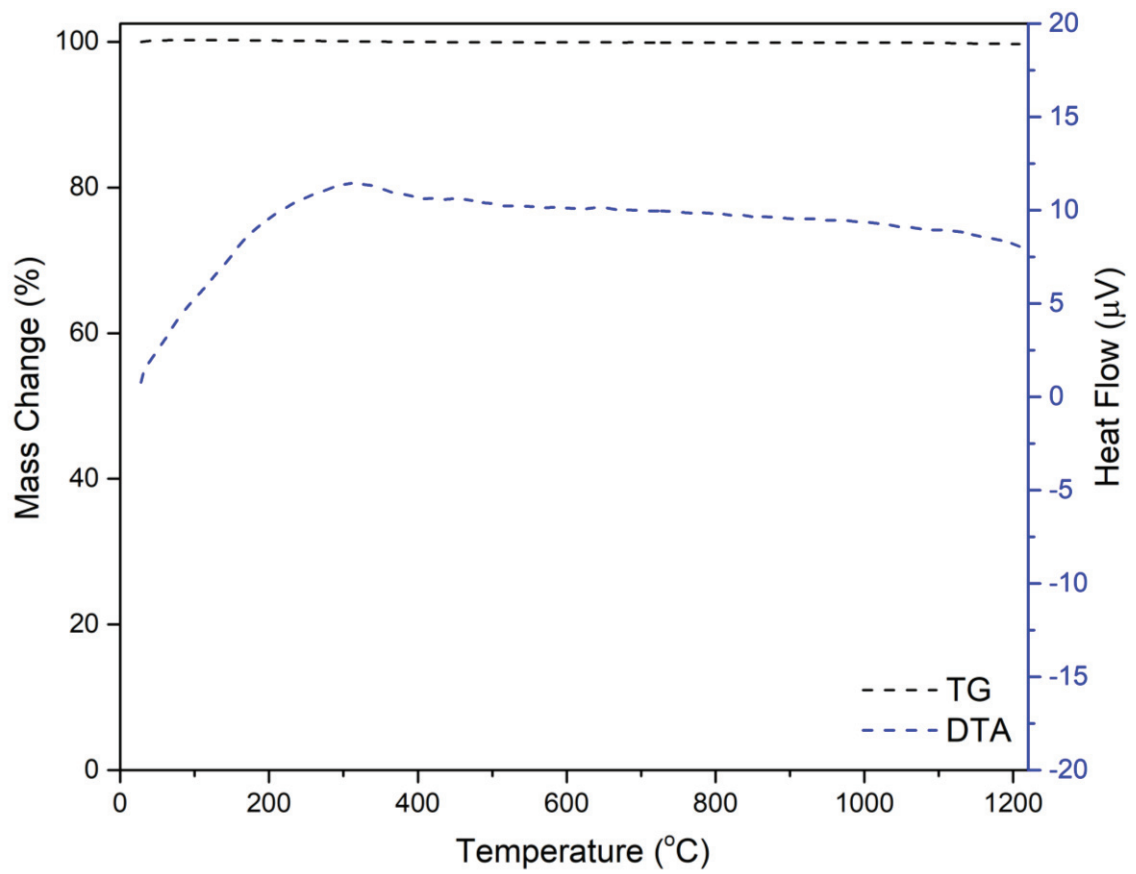
Figure 4.9. The TG-DTA curve of the powder in which the CSH sample was calcined at 1000˚C for 2h.

CHAPTER 5

CONCLUSIONS

In this thesis, refractory calcium silicates were synthesized by using recycling and economical starting materials. Firstly, the calcium source, $Ca(OH)_2$ was calcined at 1100 ˚C (5˚C.min^{-1} heating rate) for 2h just in case and kept at in oven at 90˚C constantly. Recycled glass from silicon sources was crushed, ground and sieved. The obtained recycled glass powder has a particle size of <25 μm. After these preprocesses the starting materials were pretreated by the mechanochemical method. The slurry obtained at the end of the mechanochemical process was taken into a Teflon container and sealed. The obtained slurry was then subjected to hydrothermal synthesis in the acid digestion bomb under the required conditions.

The microstructural properties of each experimental set were characterized by SEM and XRD methods. The effect of each tested parameter on the final product was examined. The rising temperatures often triggered the formation of the xonotlite phase. When the Ca/Si ratio was 0.83 or 1.00, the xonotlite phase was obtained at high temperatures (above 150˚C). Contrary to expectations, the reproducibility of the xonotlite phase was more successful than Ca/Si = 1.00 when Ca/Si = 083. This is related to the particle size and distribution of the starting materials. A batch was formed by performing multiple experiments with the test parameters from which the xonotlite phase was obtained and named as CSH sample. This CSH sample contains approximately 61% xonotlite according to quantitative analysis. According to the SEM images, the general morphology is fibrous and according to thermal analysis results, approximately 20% loss is observed up to 800˚C and this rate remains constant above 800˚C.

According to these results, xonotlite phase was obtained from recycling materials by hydrothermal methods. It is also resistant to high temperatures (above 800˚C) according to thermal analysis.

REFERENCES

1.   Kingery, W. D.; Bowen, H. K.; Uhlmann, D. R., *Introduction to ceramics*. Wiley New York: 1976.

2.   Nakahira, A.; Naganuma, H.; Kubo, T.; Yamasaki, Y., Synthesis of monolithic tobermorite from blast furnace slag and evaluation of its Pb removal ability. *Journal of the Ceramic Society of Japan* **2008,** *116* (1351), 500-504.

3.   Alawad, O. A.; Alhozaimy, A.; Jaafar, M. S.; Aziz, F. N. A.; Al-Negheimish, A., Effect of autoclave curing on the microstructure of blended cement mixture incorporating ground dune sand and ground granulated blast furnace slag. *International Journal of Concrete Structures and Materials* **2015,** *9* (3), 381-390.

4.   Kamitakahara, M.; Ohtsuki, C.; Kozaka, Y.; Ogata, S.-i.; Tanihara, M.; Miyazaki, T., Preparation of Porous Glass-Ceramics Containing Whitlockite and Diopside for Bone Repair. *Journal of the Ceramic Society of Japan* **2006,** *114* (1325), 82-86.

5.   Yue, H.; Wang, X.; Yang, Z.; Wei, C., Dynamic Hydrothermal Synthesis of Super-Low Density Xonotlite Thermal Insulation Materials from Industrial Quartz Powder. *Key Engineering Materials* **2017,** *726*.

6.   Richardson, I., The calcium silicate hydrates. *Cement and concrete research* **2008,** *38* (2), 137-158.

7.   Gabrovšek, R.; Kurbus, B.; Mueller, D.; Wieker, W., Tobermorite formation in the system CaO, C3S·SiO2·Al2O3·NaOH·H2O under hydrothermal conditions. *Cement and concrete research* **1993,** *23* (2), 321-328.

8.   Shionoya, S.; Yen, W. M., *Phosphor Handbook*. CRC Press: 1999.

9.   Khristov, T. I.; Popovich, N.; Galaktionov, S.; Soshchin, N., Calcium silicate phosphors obtained by the sol-gel method. *Glass and Ceramics* **1994,** *51* (9-10), 290-296.

10.   Dhoble, S.; Dhoble, N.; Pode, R., Preparation and characterization of Eu 3+ activated CaSiO3,(CaA)SiO3 [A= Ba or Sr] phosphors. *Bulletin of Materials Science* **2003,** *26* (4), 377-382.

11.   Nishisu, Y.; Kobayashi, M.; Ohya, H.; Akiya, T., Preparation of Eu-doped alkaline-earth silicate phosphor particles by using liquid-phase synthesis method. *Journal of alloys and compounds* **2006,** *408*, 898-902.

12.   Black, L.; Garbev, K.; Stemmermann, P.; Hallam, K. R.; Allen, G. C., Characterisation of crystalline CSH phases by X-ray photoelectron spectroscopy. *Cement and concrete research* **2003,** *33* (6), 899-911.

13.   Black, L.; Garbev, K.; Stumm, A., Structure, bonding and morphology of hydrothermally synthesised xonotlite. *Advances in Applied Ceramics* **2009,** *108* (3), 137-144.

14.   Li, X.; Chang, J., A novel hydrothermal route to the synthesis of xonotlite nanofibers and investigation on their bioactivity. *Journal of materials science* **2006,** *41* (15), 4944-4947.

15.   Lin, K.; Chang, J.; Lu, J., Synthesis of wollastonite nanowires via hydrothermal microemulsion methods. *Materials Letters* **2006,** *60* (24), 3007-3010.

16.   Saito, F.; Mi, G.; Hanada, M., Mechanochemical synthesis of hydrated calcium silicates by room temperature grinding. *Solid State Ionics* **1997,** *101*, 37-43.

17.   Brunner, G., *Hydrothermal and supercritical water processes*. Elsevier: 2014; Vol. 5.

18.   Diez-Garcia, M.; Gaitero, J. J.; Dolado, J. S.; Aymonier, C., Ultra-Fast Supercritical Hydrothermal Synthesis of Tobermorite under Thermodynamically Metastable Conditions. *Angewandte Chemie* **2017,** *129* (12), 3210-3215.

19.   García, M. D. e. Synthesis by supercritical fluids methods of advanced additions for cementitious materials. Université de Bordeaux, 2017.

20.   Sarkar, R., *Refractory technology: Fundamentals and applications*. CRC Press: 2016.

21.   Baeri, P.; Spinella, C.; Reitano, R., Fast Melting of Amorphous Silicon Carbide Induced by Nanosecond Laser Pulse. *International Journal of Thermophysics* **1999,** *20* (4), 1211-1221.

22.   Li, Z.; Bradt, R. C., Thermal Expansion and Thermal Expansion Anisotropy of SiC Polytypes. *Journal of the American Ceramic Society* **1987,** *70* (7), 445-448.

23.   Nakano, H.; Watari, K.; Kinemuchi, Y.; Ishizaki, K.; Urabe, K., Microstructural characterization of high-thermal-conductivity SiC ceramics. *Journal of the European Ceramic Society* **2004,** *24* (14), 3685-3690.

24.   Askeland, D. R.; Phule, P. P., *The science and engineering of materials*. Springer: 2003.

25.   Liu, F.; Zeng, L.; Cao, J.; Li, J., Preparation of ultra-light xonotlite thermal insulation material using carbide slag. *Journal of Wuhan University of Technology-Mater. Sci. Ed.* **2010,** *25* (2), 295-297.

26.   Wei, G.; Liu, Y.; Zhang, X.; Yu, F.; Du, X., Thermal conductivities study on silica aerogel and its composite insulation materials. *International Journal of Heat and Mass Transfer* **2011,** *54* (11-12), 2355-2366.

27.   Shaw, S.; Clark, S.; Henderson, C., Hydrothermal formation of the calcium silicate hydrates, tobermorite ($Ca_5Si_6O_{16}(OH)_2 \cdot 4H_2O$) and xonotlite ($Ca_6Si_6O_{17}(OH)_2$): an in situ synchrotron study. *Chemical Geology* **2000,** *167* (1), 129-140.

28.   Claringbull, G.; Hey, M., A re-examination of tobermorite. *Mineralogical Magazine and Journal of the Mineralogical Society* **1952,** *29* (218), 960-962.

29.   Anthony, J. W.; Bideaux, R. A.; Bladh, K. W.; Nichols, M. C., Handbook of Mineralogy, Mineralogical Society of America, Chantilly, VA 20151-1110, USA. ed: 2011.

30.   Hamid, S., The crystal structure of the 11 Ä natural tobermorite Ca2.25[Si3O7.5(OH)1.5]· 1H2O. *Zeitschrift für Kristallographie-Crystalline Materials* **1981,** *154* (1-4), 189-198.

31.   Mitsuda, T.; Taylor, H., Normal and anomalous tobermorites. *Mineral. Mag* **1978,** *42* (322), 229-235.

32.   Bell, N. S.; Venigalla, S.; Gill, P. M.; Adair, J. H., Morphological forms of tobermorite in hydrothermally treated calcium silicate hydrate gels. *Journal of the American Ceramic Society* **1996,** *79* (8), 2175-2178.

33.   Mostafa, N.; Shaltout, A.; Omar, H.; Abo-El-Enein, S., Hydrothermal synthesis and characterization of aluminium and sulfate substituted 1.1 nm tobermorites. *Journal of Alloys and Compounds* **2009,** *467* (1-2), 332-337.

34.   Yang, J.; Tan, X.; Ma, H.; Zeng, C.; Peng, H., Alkali-hydrothermal synthesis of acicular tobermorite using natural mineral K-feldspar powder. *Ferroelectrics* **2015,** *481* (1), 57-63.

35.   Youssef, H.; Ibrahim, D.; Komarneni, S.; Mackenzie, K., Synthesis of 11 Å Al-substituted tobermorite from trachyte rock by hydrothermal treatment. *Ceramics international* **2010,** *36* (1), 203-209.

36.   Connan, H.; Ray, A.; Thomas, P., Autoclaved Lime-Colloidal Silica Slurries and Formation of Tobermorite. *Journal of the Australian Ceramics Society* **2007**.

37.   Monasterio, M.; Gaitero, J. J.; Manzano, H.; Dolado, J. S.; Cerveny, S., Effect of chemical environment on the dynamics of water confined in calcium silicate minerals: natural and synthetic tobermorite. *Langmuir* **2015,** *31* (17), 4964-4972.

38.   Eℓ-Hemaly, S.; Mitsuda, T.; Taylor, H., Synthesis of normal and anomalous tobermorites. *Cement and Concrete Research* **1977,** *7* (4), 429-438.

39.   Kalousek, G. L., Crystal chemistry of hydrous calcium silicates: I, substitution of aluminum in lattice of tobermorite. *Journal of the American Ceramic Society* **1957,** *40* (3), 74-80.

40.   Reinik, J.; Heinmaa, I.; Kirso, U.; Kallaste, T.; Ritamäki, J.; Boström, D.; Pongrácz, E.; Huuhtanen, M.; Larsson, W.; Keiski, R., Alkaline modified oil shale fly ash: Optimal synthesis conditions and preliminary tests on CO2 adsorption. *Journal of hazardous materials* **2011,** *196*, 180-186.

41.   Komarneni, S.; Tsuji, M., Selective cation exchange in substituted tobermorites. *Journal of the American Ceramic Society* **1989,** *72* (9), 1668-1674.

42.   Komarneni, S.; Roy, R.; Roy, D. M., Pseudomorphism in Xonotlite and Tobermorite with Co2+ and Ni2+ Exchange for Ca2+ at 25°C. *Cement and Concrete Research* **1986,** *16* (1), 47-58.

43.   Coleman, N. J.; Li, Q.; Raza, A., Synthesis, structure and performance of calcium silicate ion exchangers from recycled container glass. *Physicochemical Problems of Mineral Processing* **2014,** *50*.

44.   Coleman, N. J., Interactions of Cd (II) with waste-derived 11 Å tobermorites. *Separation and purification technology* **2006,** *48* (1), 62-70.

45.   Coleman, N. J.; Brassington, D. S.; Raza, A.; Mendham, A. P., Sorption of Co2+ and Sr2+ by waste-derived 11 Å tobermorite. *Waste Management* **2006,** *26* (3), 260-267.

46.   Al-Wakeel, E.; El-Korashy, S.; El-Hemaly, S.; Rizk, M., Divalent ion uptake of heavy metal cations by (aluminum+ alkali metals)–substituted synthetic 1.1 nm-tobermorites. *Journal of materials science* **2001,** *36* (10), 2405-2415.

47.   Komarneni, S.; Roy, D. M. Method of storing radioactive wastes using modified tobermorite. US 4537710 United States PNNL English, 1985.

48.   McCulloch, C.; Angus, M.; Crawford, R.; Rahman, A.; Glasser, F., Cements in radioactive waste disposal: some mineralogical considerations. *Mineralogical Magazine* **1985,** *49* (351), 211-221.

49.   Lima, S.; Dias, A. S.; Lin, Z.; Brandão, P.; Ferreira, P.; Pillinger, M.; Rocha, J.; Calvino-Casilda, V.; Valente, A. A., Isomerization of D-glucose to D-fructose over metallosilicate solid bases. *Applied Catalysis A: General* **2008,** *339* (1), 21-27.

50.   Taylor, H., The identity of jurupaite and xonotlite. *Mineralogical Magazine and Journal of the Mineralogical Society* **1954,** *30* (224), 338-341.

51.   Heller, L.; Taylor, H. F., *Crystallographic data for the calcium silicates*. HM Stationery Office: 1956; Vol. 49.

52.   Hejny, C.; Armbruster, T., Polytypism in xonotlite Ca6Si6O17(OH)2. *Zeitschrift für Kristallographie-Crystalline Materials* **2001,** *216* (7), 396-408.

53.   Kalousek, G.; Mitsuda, T.; Taylor, H., Xonotlite: cell parameters, thermogravimetry and analytical electron microscopy. *Cement and Concrete Research* **1977,** *7* (3), 305-312.

54.   Shrivastava, O.; Shrivastava, R., Sr2+ uptake and leachability study on cured aluminum-substituted tobermorite–OPC admixtures. *Cement and concrete research* **2001,** *31* (9), 1251-1255.

55.   Wu, J.; Zhu, Y.-J.; Cheng, G.-F.; Huang, Y.-H., Microwave-assisted preparation of Ca6Si6O17(OH)2 and β-CaSiO3 nanobelts. *Materials Research Bulletin* **2010,** *45* (4), 509-512.

56.   Anton, O.; Eckert, A.; Eckert, A., Brake linings. Google Patents: 1991.

57.   Chan, C.-F.; Sakiyama, M.; Mitsuda, T., Kinetics of the CaO quartz H2O reaction at 120° to 180°C in suspensions. *Cement and concrete research* **1978,** *8* (1), 1-5.

58.   Zheng, Q.; Wang, W., Calcium silicate based high efficiency thermal insulation. *British ceramic transactions* **2000,** *99* (4), 187-190.

59.   Hamilton, A.; Hall, C., Physicochemical characterization of a hydrated calcium silicate board material. *Journal of Building Physics* **2005,** *29* (1), 9-19.

60.   Wei, G.; Zhang, X.; Yu, F., Thermal Conductivity of Xonotlite Insulation Material. *International Journal of Thermophysics* **2007,** *28* (5), 1718-1729.

61.   Byrappa, K.; Yoshimura, M., *Handbook of hydrothermal technology*. William Andrew: 2012.

62.   Sōmiya, S.; Roy, R., Hydrothermal synthesis of fine oxide powders. *Bulletin of Materials Science* **2000,** *23* (6), 453-460.

63.   Roy, R., Accelerating the kinetics of low-temperature inorganic syntheses. *Journal of Solid State Chemistry* **1994,** *111* (1), 11-17.

64.   Riman, R. E.; Suchanek, W. L.; Lencka, M. M. In *Hydrothermal crystallization of ceramics*, Annales de Chimie Science des Materiaux, Citeseer: 2002; pp 15-36.

65.   Morey, G. W., Hydrothermal synthesis. *Journal of the American Ceramic Society* **1953,** *36* (9), 279-285.

66.   Walton, R. I., Subcritical solvothermal synthesis of condensed inorganic materials. *Chemical Society Reviews* **2002,** *31* (4), 230-238.

67.   Hoffmann, C.; Armbruster, T., Clinotobermorite, Ca5[Si308(OH)]2·4H2O - Ca5[Si6O17]·5H2O, CSH (I) type cement mineral: determination of the substructure. *Zeitschrift fur Kristallographie* **1997,** *212*, 864-873.

68.   Henmi, C.; Kusachi, I., Clinotobermorite, Ca5Si6(O,OH)18· 5H2O, a new mineral from Fuka, Okayama Prefecture, Japan. *Mineralogical Magazine* **1992,** *56* (384), 353-358.

69.   Merlino, S.; Bonaccorsi, E.; Armbruster, T., The real structure of tobermorite 11Å: normal and anomalous forms, OD character and polytypic modifications. *European Journal of Mineralogy* **2001,** *13* (3), 577-590.

70.   Tränkle, S.; Jahn, D.; Neumann, T.; Nicoleau, L.; Hüsing, N.; Volkmer, D., Conventional and microwave assisted hydrothermal syntheses of 11 Å tobermorite. *Journal of Materials Chemistry A* **2013,** *1* (35), 10318-10326.

71.   Milestone, N.; Ahari, G. K., Hydrothermal processing of xonotlite based compositions. *Advances in Applied ceramics* **2007,** *106* (6), 302-308.

72.   Liu, F.; Zeng, L. K.; Cao, J. X.; Zhu, B.; Yuan, A. In *Hydrothermal synthesis of xonotlite fibers and investigation on their thermal property*, Advanced Materials Research, Trans Tech Publ: 2010; pp 841-843.

73.   Hartmann, A.; Schulenberg, D.; Buhl, J.-C., Investigation of the transition reaction of tobermorite to xonotlite under influence of additives. *Advances in Chemical Engineering and Science 5 (2015), Nr. 2* **2015,** *5* (2), 197-214.

74.   Hartmann, A.; Schulenberg, D.; Buhl, J.-C., Synthesis and Structural Characterization of CSH-Phases in the Range of C/S= 0.41-1.66 at Temperatures of the Tobermorite Xonotlite Crossover. *Journal of Materials Science and Chemical Engineering 3 (2015), Nr. 11* **2015,** *3* (11), 39-55.

75.   Mostafa, N. Y.; Garib, R. A.; Heiba, Z.; Abd-Elkader, O. H.; Al-Majthoub, M., Synthesis of pure zeolite P2 from calcium silicate hydrate; tobermorite. *Oriental Journal of Chemistry* **2015,** *31* (2), 1051-1056.

76.   Singh, S. P.; Karmakar, B., Mechanochemical synthesis of nano calcium silicate particles at room temperature. *New journal of glass and ceramics* **2011,** *1* (2), 49-52.

77.   Spudulis, E.; Šavareika, V.; Špokauskas, A., Influence of hydrothermal synthesis condition on xonotlite crystal morphology. *Materials Science* **2013,** *19* (2), 190-196.

78.   Hamid, S., Electron microscopic characterization of the hydrothermal growth of synthetic 11Å tobermorite (Ca6Si6O18· 4H2O crystals. *Journal of Crystal Growth* **1979,** *46* (3), 421-426.

79.   Hara, N.; Chan, C.; Mitsuda, T., Formation of 14Å tobermorite. *Cement and Concrete Research* **1978,** *8* (1), 113-115.

80.   Flint, E. P.; McMurdie, H. F.; Wells, L. S., Formation of hydrated calcium silicates at elevated temperatures and pressures. *Journal of Research of the National Bureau of Standards* **1938,** *21*, 617-638.

81.   Yazdani, A.; Rezaie, H. R.; Ghassai, H., Investigation of hydrothermal synthesis of wollastonite using silica and nano silica at different pressures. *Journal of Ceramic Processing Research* **2010,** *11* (3), 348-353.

82.   Speakman, K., The stability of tobermorite in the system CaO-SiO2-H2O at elevated temperatures and pressures. *Mineralogical Magazine and Journal of the Mineralogical Society* **1968,** *36* (284), 1090-1103.

83.   Tantawy, M.; Shatat, M.; El-Roudi, A.; Taher, M.; Abd-El-Hamed, M., Low temperature synthesis of belite cement based on silica fume and lime. *International scholarly research notices* **2014,** *2014*.

84.   Garbev, K.; Gasharova, B.; Beuchle, G.; Kreisz, S.; Stemmermann, P., First Observation of α-Ca2[SiO3(OH)](OH)–Ca6[Si2O7][SiO4](OH)2 Phase Transformation upon Thermal Treatment in Air. *Journal of the American Ceramic Society* **2008,** *91* (1), 263-271.

85.   Ishida, H.; Yamazaki, S.; Sasaki, K.; Okada, Y.; Mitsuda, T., α-Dicalcium Silicate Hydrate: Preparation, Decomposed Phase, and Its Hydration. *Journal of the American Ceramic Society* **1993,** *76* (7), 1707-1712.

86.   Wu, J.; Zhu, Y.-J., Hydrothermal synthesis of Ca2(SiO3)(OH)2 microbelts and their transformation to β-Ca2SiO4 microbelts by microwave heating. *Materials Letters* **2009,** *63* (9), 761-763.

87.   Okada, Y.; Ishida, H.; Mitsuda, T., Thermal decomposition of tricalcium silicate hydrate. *Journal of the American Ceramic Society* **1994,** *77* (9), 2277-2282.

88.   Qian, G.; Xu, G.; Li, H.; Li, A., Mg-xonotlite and its coexisting phases. *Cement and concrete research* **1997,** *27* (3), 315-320.

89.   Garbev, K.; Beuchle, G.; Schweike, U.; Merz, D.; Dregert, O.; Stemmermann, P., Preparation of a Novel Cementitious Material from Hydrothermally Synthesized C–S–H Phases. *Journal of the American Ceramic Society* **2014,** *97* (7), 2298-2307.

90.   Arthur, L. F.; Rochelle, G. T., Preparation of calcium silicate absorbent from recycled glass. *Environmental Progress & Sustainable Energy* **1998,** *17* (2), 86-91.

91.   Riti, P.; Vulpoi, A.; Ponta, O.; Simon, V., The effect of synthesis route and magnesium addition on structure and bioactivity of sol–gel derived calcium-silicate glasses. *Ceramics International* **2014,** *40* (9), 14741-14748.

92.   Wu, C.; Zreiqat, H., Porous bioactive diopside (CaMgSi2O6) ceramic microspheres for drug delivery. *Acta biomaterialia* **2010,** *6* (3), 820-829.

93.	The photograph and schematics of the autoclave https://www.parrinst.com/download/37527/ (Accessed April 9, 2019).

94.	Paufler, P., R. A. Young (ed.). The Rietveld Method. International Union of Crystallography. Oxford University Press 1993. 298 p. ISBN 0–19–855577–6. *Crystal Research and Technology* **1995,** *30* (4), 494-494.

95.	Bortolotti, M.; Lutterotti, L.; Pepponi, G., Combining XRD and XRF analysis in one Rietveld-like fitting. *Powder Diffraction* **2017,** *32* (S1), S225-S230.

96.	Popa, N. C.; Balzar, D., An analytical approximation for a size-broadened profile given by the lognormal and gamma distributions. *Journal of Applied Crystallography* **2002,** *35* (3), 338-346.

97.	Delhez, R.; de Keijser, T. H.; Mittemeijer, E. J., Determination of crystallite size and lattice distortions through X-ray diffraction line profile analysis. *Fresenius′ Zeitschrift für analytische Chemie* **1982,** *312* (1), 1-16.

98.	Levinskas, R.; Lukošiūtė, I.; Baltušnikas, A.; Kuoga, A.; Luobikienė, A.; Rodriguez, J.; Cañadas, I.; Brostow, W., Modified xonotlite–type calcium silicate hydrate slabs for fire doors. *Journal of fire sciences* **2018,** *36* (2), 83-96.

99.	Crouch-Baker, S.; Huang, C.; Huggins, R., Rationalization of the electrochemical behavior of transition metal oxide positive electrode materials at room temperature. *Proc. Electrochem. Soc* **1988**, 88-6.

100.	Vakifahmetoglu, C., Zeolite decorated highly porous acicular calcium silicate ceramics. *Ceramics International* **2014,** *40* (8, Part A), 11925-11932.

101.	Núñez-Rodríguez, L. A.; Tiburcio-Munive, G. C.; Valenzuela-García, J. L.; Gómez-Álvarez, A.; Encinas-Romero, M. A., Evaluation of Bioactive Properties of α and β Wollastonite Bioceramics Soaked in a Simulated Body Fluid. *Journal of Biomaterials and Nanobiotechnology* **2018,** *9* (3), 720-726.